ARMY RESEARCH LABORATORY

Coupling Meteorology to Acoustics in Forests

by Arnold Tunick

ARL-MR-538 September 2002

The findings in this report are not to be construed as an official Department of the Army position unless so designated by other authorized documents.

Citation of manufacturer's or trade names does not constitute an official endorsement or approval of the use thereof.

Destroy this report when it is no longer needed. Do not return it to the originator.

Army Research Laboratory
Adelphi, MD 20783-1197

ARL-MR-538 **September 2002**

Coupling Meteorology to Acoustics in Forests

Arnold Tunick
Computational and Information Sciences Directorate, ARL

Acknowledgments

The author would like to thank Sam Chang, Ronald Meyers, John Noble, and Keith Wilson of the U.S. Army Research Laboratory for offering helpful comments.

Contents

List of Figures

List of Tables

1. Introduction

The U.S. Army's soldiers will make unprecedented use of advanced systems and sensors on the Future Combat System's (FCS's) battlefield (see http://www.darpa.mil/fcs/index.html, 03/26/02). This will include the use of low-cost, non-line-of-sight acoustic sensor systems for the surveillance, detection, identification, classification, and tracking of military targets (i.e., Fong and Srour 1994; Rosenthal and Stevens 1994; Srour and Robertson 1995; Young et al. 1999; Becker and Güdesen 2000; and Mays and Price 2000). Most new U.S. Army acoustic systems use unattended microphone sensors to construct small ground-based beam-forming arrays to determine the line-of-bearing angle of sound-emitting targets [e.g., the remote netted acoustic/seismic sensor array (RNADS) (Thompson and Scherer 1991; Carnes and Morgan 1995; Wilson 1997; Eom et al. 1999; Lopez et al. 1999; Wellmann and Srour 1999; Wellman 1999; Depireux and Shamma 2000; and Mays and Vu 2000)]. Hence, the U.S. Army has a growing interest to implement accurate and reliable computer models for determining point-to-point acoustic transmission (West et al. 1991; West et al. 1992; Wilson 1993; Noble and Marlin 1995; and Wilson 2000). At the same time, the retrieval and interpretation of acoustic signals in diverse microclimate area, (e.g., in and around forests, hilly terrain, arid deserts, coastal areas, or in cities) is greatly influenced by turbulence and refraction effects caused by finer scale atmospheric motions over varying topography and surface energy budgets (Smith 1989; Auvermann and Goedecke 1993; Auvermann et al. 1995; Goedecke et al. 1997; Wilson 1998ab; Goedecke et al. 2000; and Auvermann 2001). We expect, therefore, that improved physics-based theory and computer models for meteorology coupled to acoustics will contribute important information on the performance of critical battlefield systems.

2. Meteorology and Acoustics

The topic of this report is the coupling of meteorology to acoustics in forests. We focus on deriving estimates for sound speed, from which it is possible to determine sound intensity and attenuation. The value for the speed of sound may be computed from Newton's 2nd Law as follows (Fleagle and Businger 1963): The change in pressure (dp) over a unit cross-sectional area of a fluid containing a sound wave (i.e., between the plane of compression and plane of rarefaction) can be expressed as

$$dp = -\rho \, ds \, \frac{dc}{dt} \, , \tag{1}$$

where ρ is the density of the fluid medium, ds is an increment of distance in the direction of propagation, and dc is the change in sound speed over an increment of time, dt. Equation (1) can be re-written as

$$-\alpha \, dp = c \, dc \tag{2}$$

because $\alpha = \rho^{-1}$ is specific volume and $\frac{ds}{dt} = c$. The volume (V) of fluid moving through a unit cross-sectional area of a fluid medium is $V = c\,dt$ so that any fractional change in this volume ($\frac{dV}{V}$) can be equated to a fractional change in sound speed (i.e., $\frac{dV}{V} = \frac{dc}{c}$). Also, the volume of fluid is proportional to its specific volume (i.e., $V = M\,\alpha$, and $dV = M\,d\alpha$,) which yields $\frac{dV}{V} = \frac{dc}{c} = \frac{d\alpha}{\alpha}$. Therefore, equation (2) can be re-written as

$$\frac{dp}{d\alpha} = -\frac{c^2}{\alpha^2} \quad . \tag{3}$$

Based on the principles of thermodynamics and the behavior of ideal gases, one expects that this ratio of pressure change to volume change will depend on the amount of heat transferred between adjacent fluid elements undergoing either compression or expansion. Textbooks such as Fleagle and Businger (1963) consider the following two extreme cases: Heat transfer is sufficiently rapid such that no temperature gradient exists in the fluid (i.e., temperature remains constant during the process); or heat flux is negligible and the process is adiabatic. To demonstrate the first case we can expand the equation of state (EOS) (i.e., $p\ \alpha = \frac{RT}{M}$) where R = 8314.32 $J\,mol^{-1}\,K^{-1}$ is the universal gas constant and M is molecular mass, for constant temperature (T) as

$$p\,d\alpha + \alpha\,dp = 0 \ , \tag{4}$$

so that substitution into equation (3) yields,

$$c^2 = p\,\alpha = \frac{RT}{M} \quad \text{or} \quad c = \sqrt{\frac{RT}{M}} \ . \tag{5}$$

This sound speed for isothermal (constant temperature) expansion is often called the 'Newtonian' velocity of sound.

In the second case, where pressure and volume change across elements of a fluid medium, transmitting sound waves are considered to occur under adiabatic conditions. Then the value for the speed of sound may be computed from the 1st Law of Thermodynamics as follows (Fleagle and Businger 1963):

$$dH = dQ + p\,d\alpha \ , \tag{6}$$

where dH is the incremental amount of heat added to a given system, $dQ = c_v T$ is the internal energy of the system, where c_v is the specific heat at constant volume of a fluid (in units $J\ Kg^{-1}\ K^{-1}$), and $p\,d\alpha$ is the work or change in energy of the system as it undergoes expansion or compression. Because an adiabatic process by definition is one in which no heat is added or lost to a given system (i.e., $dH = 0$) and by definition an isentropic process is that where no entropy is added or lost (i.e., $dS_e = \frac{dH}{T} = 0$) where dS_e is the differential of specific entropy, then from the EOS and equation (6) we can derive the following expression:

$$0 = c_v \frac{dT}{T} + \frac{R}{M}\frac{d\alpha}{\alpha} \quad . \tag{7}$$

Because $\frac{R}{M} = c_p - c_v$, where c_p is the specific heat at constant pressure of a fluid (in units $J\,Kg^{-1}\,K^{-1}$), then through some algebraic manipulation, equation (7) can be re-written as,

$$0 = \frac{c_p}{c_v}\frac{d\alpha}{\alpha} + \frac{dp}{p} \quad . \tag{8}$$

Returning to the problem to define the ratio of pressure change to volume change for an adiabatic (or isentropic) process, we have from equation (8),

$$\frac{dp}{d\alpha} = -\frac{c_p}{c_v}\frac{p}{\alpha} \quad , \tag{9}$$

so that substitution into equation (3) yields,

$$c = \sqrt{\frac{\gamma\, RT}{M}} \quad , \tag{10}$$

where $\gamma = \frac{c_p}{c_v}$ is the ratio of specific heats. Equation (10) for the speed of sound (c) has been found to agree closely with observations. For application to outdoor acoustics, Wong and Embleton (1984, 1985) have deduced the ratio of specific heats and molar mass ($\frac{\gamma}{M}$) as a function of temperature and humidity in the form,

$$\frac{\gamma}{M} = 0.04833 + (h - 0.023)A_t \quad , \tag{11}$$

where $A_t = 9.2 \times 10^{-5} + 5.5 \times 10^{-6} t + 4.25 \times 10^{-7} t^2$, h is humidity (in the range 0.0 to 1.0) and t is air temperature in degrees Celsius. From equation (11), Wong (1986) has calculated the value for the speed of sound in standard dry air at 0 °C and a barometric pressure of 1013.25 mbar to be $c_o = 331.29\ ms^{-1}$.

In addition, to account for increases and decreases in sound speed due to variations in wind velocity, it is useful to define an effective sound speed from the following expression given by Noble and Marlin (1995) and Osteshev (1997):

$$c_{eff} = c_o + \bar{u} \cos\left(\theta_w - \pi - \theta_{S,R}\right) \quad , \tag{12}$$

where $\bar{u}$ is the mean of the horizontal wind, θ_w is the bearing of the wind from North, θ_R is the bearing of the receiver from the source, and $\bar{u}\ \cos\left(\theta_w - \pi - \theta_{S,R}\right)$ is the component of the sound speed along the direction of propagation from the source to the receiver (see Figure 1). As discussed in Osteshev (1997), the effective sound speed in equation (12) is valid only for nearly horizontal propagation angles (Wilson 2002).

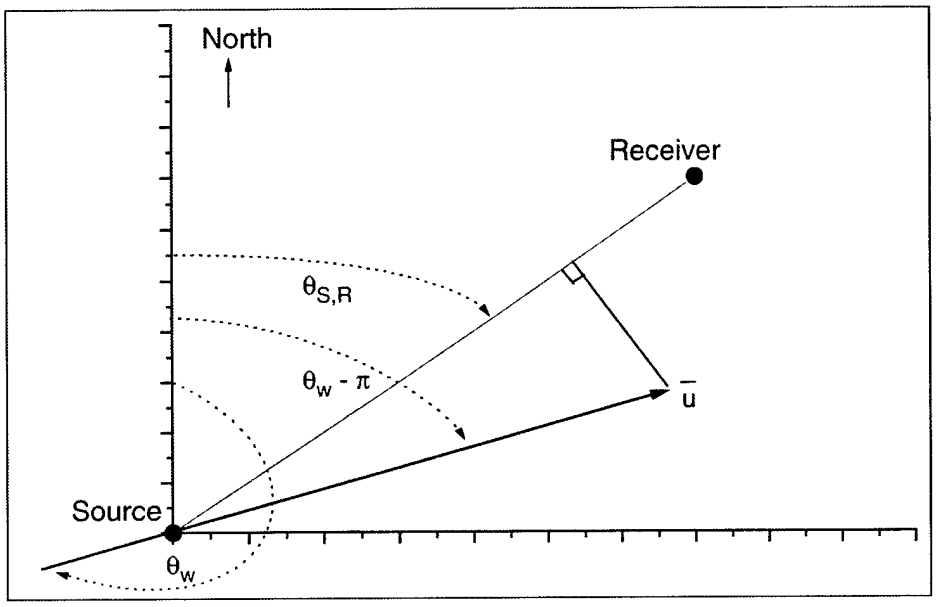

Figure 1. Geometry schematic for the expression $c_{eff} = c_0 + \bar{u}\ \cos(\theta_w - \pi - \theta_{S,R})$. where c_{eff} is the effective sound speed that includes the sound speed component due to the mean wind along the path of propagation.

The effective speed of sound in equation (12) will also vary with height (z) above ground level as a function of the profiles of air temperature, humidity, and wind velocity. Generally, sound speed differences across vertical layers will cause acoustic waves to be refracted upward if the effective sound speed decreases with height and refracted downward if sound speed increases with height. Over flat and uniform terrain, wind velocity profiles through the surface layer ($z \leq 50$ m) are generally increasing (logarithmically) with height and are easily predicted via traditional profile theory (Monin and Obukhov 1954). Likewise, temperature profiles can be extrapolated upward through the surface layer for homogeneous and steady state conditions. In contrast, computer models to describe meteorological profiles within and above forests are not as easily determined or well known. Therefore, the remainder of this report will present an overview of selected past research on meteorology in forests to examine the calculation of the speed of sound through the atmosphere in the forest environment for military acoustic applications. Our objective is to evaluate meteorological models for estimating wind speed and temperature profiles within and above forests to determine which models are most applicable in representing mechanical and thermodynamic influences on the speed of sound in the forest environment.

3. Vertical Profiles of Wind Speed in Forests

An extensive survey of literature shows that the study of winds in forests has been motivated primarily by scientific interests to better understand surface exchanges of heat, moisture (water vapor), and carbon dioxide. Such properties not only influence regional and local climate, but also affect the forest ecosystem, growth, and regeneration. Others have retrieved wind related data in forests for the study of transport, diffusion, and deposition of air-borne pollutants and aerial sprays. At the same time, scientists have found it necessary to assess the impact of wind damage on trees and tree harvests by severe storms (e.g., Coutts and Grace 1995).

3.1 Meteorological Measurements

Numerous vertical wind speed profiles within and above forest canopies have been retrieved through meteorological measurements and reported by various authors (e.g., Allen 1968; Bergen, 1971; Martin 1971; Oliver 1971; Raynor 1971; Denmead and Bradley 1985; Amiro and Davis 1988; Baldocchi and Hutchinson 1988; Baldocchi and Meyers 1988; and Lee and Black 1995). The main features of wind speed profile structure within and above a forest stand (Figure 2) on clear days are as follows: 1) a low-level wind maximum at 0.1 to 0.3h, where the live canopy (i.e., branches and leaves) extends from about $0.3h \leq z \leq h$, where h is the height of the canopy top; 2) a layer of minimum wind speed at 0.6 to 0.8h, which coincides with the region of maximum leaf area density; and 3) a diurnal time maximum of wind speed, which extends through the entire canopy in the early afternoon. Minimum wind speeds through the tree crown have been associated with the zero-plane displacement height, d. Zero-plane displacement determined from various experiments in pine forests have fallen within the range $0.70 - 0.76h$ (Bergen 1971; Raynor 1971; Oliver 1971; and Lee and Black 1993). Bergen (1971) remarked that similar features in profile structure have resulted from airflow measurements through modeled forests in wind tunnels (e.g., Meroney 1968; Sadeh et al., 1971; and Chen et al., 1995). Oliver (1971) commented that over the course of his fieldwork no significant variations in profile shape were found for different mean wind speeds.

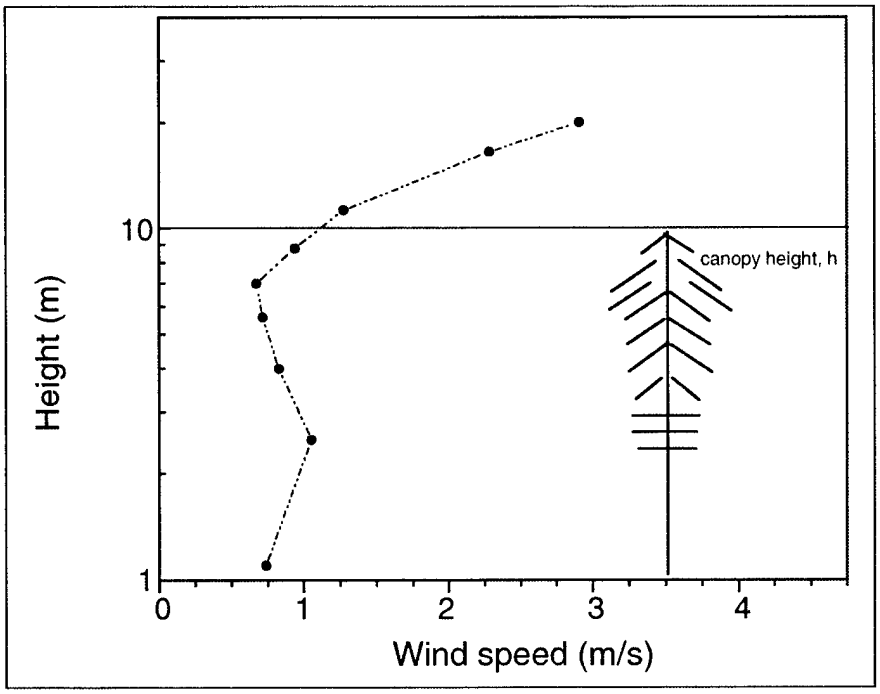

Figure 2. Typical vertical wind speed profile structure within and above a forest stand (based on Bergen 1971).

However, in a recent measurement study of the vertical distribution of wind speed in a dense maize canopy (h = 1.7m), Jacobs, et al. (1995) found a (sub-canopy) local velocity maxima around $0.1h$. Similarly, Lee and Black (1993) reported secondary maxima in wind speed at $0.12h$ for a relatively uniform expanse of tall pine trees (h = 16.7m, on average). Hence, the height of the subcanopy wind maxima is strongly influenced by the shape, density, and leaf area distribution of the trees.

Massman (1982) studied vertical distributions of foliage (i.e., needle surface area, for nine old-growth Douglas fir crowns and one old-growth sugar pine) and showed several comparisons of data and distribution models to estimate the observed profiles. Analysis of Massman's data and other leaf area models reported in the literature, such as Meyers (1987), Paw U and Meyers (1989) and Meyers et al. (1998), suggested that forest canopies regularly conform to one of three general leaf area distribution profiles (Figure 3). They found that leaf area distributions are not always symmetric about the layer of maximum foliage density, like Profile 1, but are more often skewed upward toward the top of the forest canopy, as shown in Profile 2 and Profile 3. In turn, Meyers et al. (1998) presented useful parameterizations for roughness length (z_0) and a zero-plane displacement height (d) as a function of leaf area density, based their previous works as well as the earlier work of Shaw and Periera (1982),

$$d = h\left(0.05 + \frac{LAI^{0.2}}{2} + \frac{(P-1)}{20}\right); \tag{13}$$

and

$$z_0 = h\left(0.23 - \frac{LAI^{0.25}}{10} - \frac{(P-1)}{67}\right), \tag{14}$$

where LAI is the leaf area index and $P = 1$, 2, or 3 correspond to one of the three general profile shapes described in Figure 1.

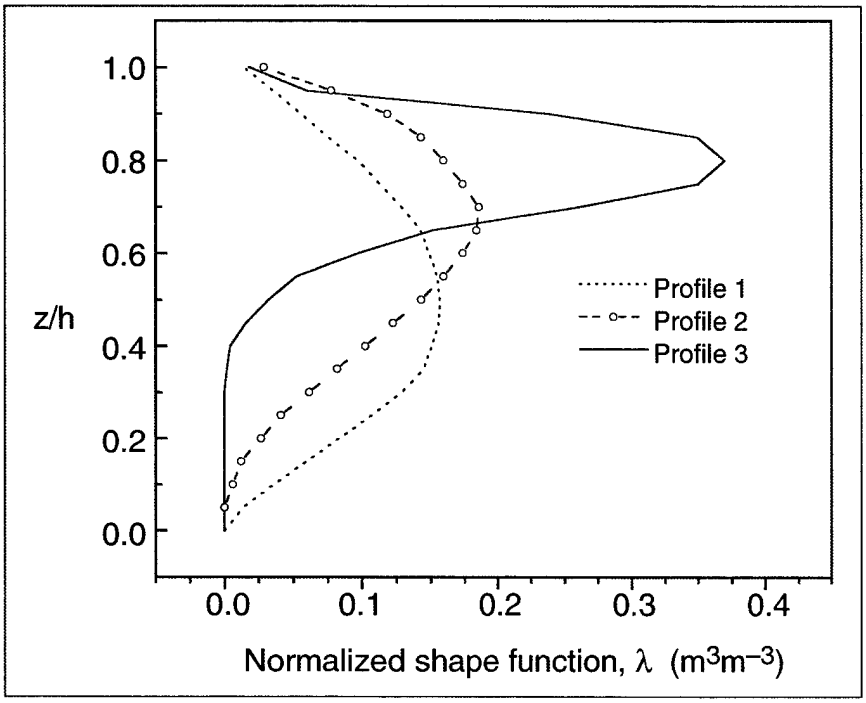

Figure 3. Normalized vertical profiles of leaf area distribution for forest canopies where $A(z) = \lambda(z) \cdot LAI$ (based on Meyers et al. 1998; and Albertson et al. 2001).

By definition, the leaf area index is $LAI = \int_0^h A(z)\, dz$, where $A(z)$ is the leaf area density through the small vertical layer between z and $z + dz$ per unit surface area of ground below (Munn 1966). Values for leaf area index for forests vary, but have been reported most often in the range LAI=1 to 5 (Pielke 1984; Kaimal and Finnigan 1994; Finnigan and Brunet 1995; and Pyles et al. 2000). Roughness length (z_0), in contrast, is the quantity that varies in the following manner: z_0 is ~10^{-4} m over snow, sand, dry lakebeds, or concrete, ~10^{-2} m over soils, ~0.1 m over farmlands, tall grass, or shrubs, and ~1.0 m for orchards and forests (Oke 1978 and Pielke 1984). Typical values for these types of data also can be found in a table compiled by Rachele and Tunick (1994).

3.2 Wind Speeds Above an Idealized (Uniform) Forest Stand

Such profile characterizations assume (idealized) steady and horizontally homogeneous conditions over large areas. Initially, therefore, we may assume that at some height above tall roughness elements, wind speed profiles are similar in form to those described for lower roughness

elements (Busch 1973). As a result, wind speed profile structure above an idealized forest stand can be described as

$$\frac{\partial \overline{U}}{\partial z} = \frac{u_*}{k(z-d)}\phi_m \quad , \tag{15}$$

where $\overline{U}$ is the mean wind speed, $u_* = \sqrt{\frac{\tau}{\rho}}$ is the friction velocity, $\frac{\tau}{\rho} = -\overline{u'w'}$ is the vertical turbulent shearing stress, ρ is air density, k is Karman's constant ($k \sim 0.4$), d is zero-plane displacement, and ϕ_m is a non-dimensional parameter that is a function of atmospheric (thermal and mechanical) stability (Monin and Obukhov 1954 and Dyer 1974). Then based on the work of Panofsky (1963) and Benoit (1977), the mean vertical profiles of wind speed above forests can be determined as

$$\overline{U} - \overline{U}_h = \frac{u_*}{k}\left[\ln\left(\frac{z-d}{z_0}\right) - \psi_m\right] \quad , \tag{16}$$

where ψ_m is referred to as the diabatic influence function, which modifies the standard log-law wind profile for non-adiabatic lapse rate conditions (Paulson 1970 and Webb 1970).

Alternately, Martin (1971) applied a power-law exponent model to determine the influence of stability and site characteristics on profile structure in the layer above the canopy top,

$$\overline{U}_{z_2} = \overline{U}_{z_1}\left(\frac{z_2 - d}{z_1 - d}\right)^P \quad , \tag{17}$$

where $\overline{U}_{z_1}$ and $\overline{U}_{z_2}$ are the wind speeds (in units m/s) at heights z_1 and z_2 above the canopy top (h), and the exponent $0 < P \leq 1$ is determined from measured wind speed data for different times of day (i.e., for varying thermal stability). Several authors have provided tables to give examples of predicted and observed values for the power-law exponent, P, for various sites (DeMarrais 1959; Touma 1977; and Irwin 1979).

Immediately above the forest stand, however, there is a region within which modified log-law and power-law exponent models tend to depart from the observed profiles (Garratt 1992). The so-called transition layer, or roughness sub-layer, transfers additional momentum from the wind flow towards the surface due to canopy-top generated turbulence (Garratt 1992; Kaimal and Finnigan, 1994; and Zoumakis 1994). Garratt (1980, 1992) contends that atmospheric observations from numerous field studies supports the following empirical modification to the wind speed and wind shear profiles for tall crops and trees

$$\frac{\partial \overline{U}}{\partial z} = \frac{u_*}{k(z-d)}\,\phi_m\,\phi_m^* \quad , \tag{18}$$

where

$$\phi_m^* = \exp\left[-0.7\left(1 - \frac{z}{z_*}\right)\right] \quad \text{for} \quad z < z_* \quad , \tag{19}$$

where $z > h$ is height above ground level, and z_* is the depth of the roughness sub-layer. Values of $\frac{z_*}{z_0}$ for stable and unstable conditions are reported to vary between 10 and about 150 and have been found to be a function of roughness density, (i.e., lower values corresponding to more dense canopies and vise versa [Garratt 1980, 1992]). As a result, the depth of the transition layer for typical forests ($z_0 \sim 1.0$ m) was found to vary according to $z_* \sim 3\delta$, where δ is tree spacing (δ = 10–30 m, possibly). Alternately, Arya (2001) suggests that the top of the transition sublayer could be estimated as $z_* = 1.5h$ to $2.5h$, also depending on the roughness density. Equation (18) is integrated to yield the mean vertical profiles of wind speed through the transition sublayer as

$$\overline{U} - \overline{U}_h = \frac{u_*}{k}\left[\ln\left(\frac{z-d}{z_0}\right) - \psi_m + \psi_m^*\right] \quad \text{for} \quad z < z_* \ , \tag{20}$$

where $\psi_m^* = f\left(\phi_m^{*-1}\right)$ is defined in the same manner as ψ_m (i.e., $\psi_m = 2\ln\left(\frac{1+x}{2}\right) + \ln\left(\frac{1+x^2}{2}\right) - 2\tan^{-1}x + \frac{\pi}{2}$, where $x = \phi_m^{-1}$; see (Paulson 1970) and (Webb 1970). ψ_m^* is a positive quantity and gives the excess in wind speed due to enhanced canopy-top turbulence, which in effect, decreases the vertical profile gradient (see Figure 4). In a calculation described by Zoumakis (1994), the modeled forest height, displacement, and roughness were given as h = 18.5 m, d = 11.3 m, and z_0 = 1.2 m, respectively, which resulted in a value for the depth of the transition layer of z_* = 32 m.

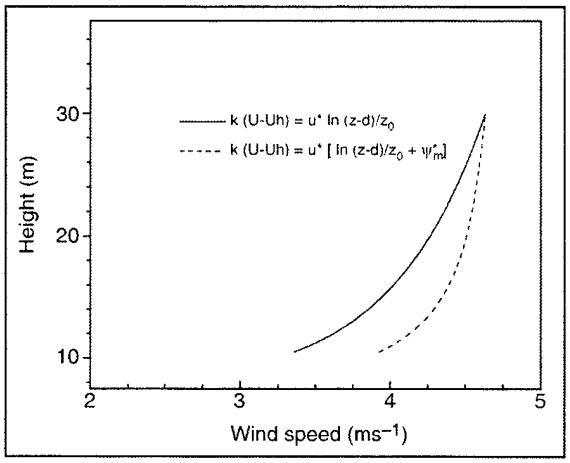

Figure 4. Mean vertical profiles of wind speed through the transition sublayer for neutral (adiabatic) conditions using equation (20) to account for enhanced canopy-top generated turbulence. The log-law profile is modified by ψ_m, which gives an excess in wind speed and decreases the profile gradient. For this example, h = 10 m, z_0 ~ 0.74 m, u_* = 0.5 ms^{-1}, and z_* = 30 m.

3.3 Wind Speeds Within an Idealized (Uniform) Forest Stand

From conservation of momentum for steady state, homogeneous (non-advective and equilibrium) conditions, air flow within the canopy and subcanopy layers of an idealized (uniform) forest stand is often described as the balance of momentum flux divergence ($\frac{\partial \overline{u'w'}}{\partial z}$), horizontal pressure gradient ($\frac{\partial \overline{p}}{\partial x}$), and drag due to friction ($\frac{1}{2}C_d A\ \overline{U}^2$), which is the drag imparted to the wind flow by the canopy leaves and branches (Barr 1971; Shaw 1977; and Shinn 1971). The equation for wind flow within the forest canopy, therefore, is often expressed as

$$\frac{\partial \overline{u'w'}}{\partial z} = -\frac{\partial \overline{p}}{\partial x} - \frac{1}{2}C_d A\ \overline{U}^2 , \tag{21}$$

where $C_d = \frac{2u_*^2}{\overline{U}^2}$ is the surface drag coefficient (Munn 1966); $u_*^2 = \frac{\tau}{\rho}$ (i.e., the friction velocity squared, is a measure of the surface stress associated with the drag); $\overline{U}^2$ is the mean wind velocity squared; and A (as defined above) is the leaf area density for the forest canopy. The assumption of horizontal homogeneity also implies that within the canopy itself, far enough away from leading or trailing edge transition zones (i.e., in equilibrium flow), there are no appreciable changes in the horizontal pressure gradient; in other words, the mean horizontal wind speeds do not decelerate, $\frac{\partial \overline{U}}{\partial x} < 0$, or accelerate, $\frac{\partial \overline{U}}{\partial x} < 0$, and $\frac{\partial \overline{p}}{\partial x}$ is approximately constant. Also, through scale analysis, one finds that the accelerations due to the horizontal pressure gradient forces are on the order of 10^{-4} ms^{-2}. Therefore, in the upper part of the canopy, when conditions are such that turbulent shearing stresses and drag forces are dominant, the following expression holds:

$$\frac{\partial \overline{u'w'}}{\partial z} = -\frac{1}{2}C_d A\ \overline{U}^2 . \tag{22}$$

Solving this complex equation* results in the well known exponential or extinction profile for wind speeds in the upper portion of the forest canopy, which can be written as described by Inoue (1963), Cionco (1965), Shinn (1971), and Albini (1981) as

$$\overline{U} = \overline{U}_h \exp\left[-n\left(1 - \frac{z}{h}\right)\right], \tag{23}$$

*By the mixing length hypothesis, the turbulent shearing stress is related to the mean velocity gradient so that the dependent variable on the left hand side of equation (22) can be rewritten as $\overline{u'w'} = -l^2\left|\frac{\partial \overline{U}}{\partial z}\right|\frac{\partial \overline{U}}{\partial z} = -l^2\left(\frac{\partial \overline{U}}{\partial z}\right)^2$. Its derivative with respect to height yields $-2l^2\frac{\partial \overline{U}}{\partial z}\frac{\partial^2 \overline{U}}{\partial z^2} = -\frac{1}{2}C_d A\overline{U}^2$ or $\frac{\partial \overline{U}}{\partial z}\frac{\partial^2 \overline{U}}{\partial z^2} = -\frac{C_d A}{4l^2}\overline{U}^2$. From this expression, one can show that equation (23) is a satisfactory result.

where $\overline{U}_h$ is the mean wind speed at the forest top, $n = h\left(\frac{C_d A}{4l^2}\right)^{\frac{1}{3}}$ is the extinction coefficient, which is a function of leaf area density and surface drag, and l is mixing length, often used in parameterizations to estimate the momentum flux (i.e., $\overline{u'w'} = -l^2\left|\frac{\partial \overline{U}}{\partial z}\right|\frac{\partial \overline{U}}{\partial z}$). The extinction coefficient, n also has been referred to as the canopy flow index (see Table 1), the values of which have been determined experimentally for various forest canopy types (Shinn 1971). Alternately, Meyers (1987) and Meyers et al. (1998) suggest the following modification to equation (23)

$$\overline{U} = \overline{U}_h \exp\left[-\lambda\left(1 - \frac{z}{h}\right)^{\beta}\right], \tag{24}$$

where $\lambda = LAI$ and $\beta = 1 - \left(\frac{P-1}{4}\right)$, where $P = 1$, 2, or 3 correspond to one of the three general profile shapes (leaf area distributions) for forest canopies, as discussed earlier. Finally, the extinction profiles described here could be similarly applied to estimate the wind-turning angle [i.e., $\alpha_0 = \tan^{-1}\left(\frac{\overline{v}}{\overline{u}}\right)$] from the subcanopy wind velocity components $\overline{u} = \overline{U}\sin\alpha_0$ and $\overline{v} = \overline{U}\cos\alpha_0$ (Shinn 1971).

Table 1. Canopy flow indices determined experimentally at various forest sites, as reported by Shinn (1971).

Gum-Maple	4.42 ± 1.05
Maple-Fir	4.03 ± 0.69
Jungle	3.84 ± 1.52
Spruce	2.74 ± 1.29
Oak-Gum	2.68 ± 0.66

In the lower portion of the forest canopy (i.e., through the open trunk spaces where air flow is considerable less restricted) wind speeds are said to be influenced by drag at the ground surface, thermal stability (inverted or convective), wind gusts that penetrate through clearings at the forest top; and to a lesser extent (in a large uniform expanse), horizontal advection (Shinn 1971; Shaw 1977; and Holland 1989). In addition, a low-level wind maximum is often observed at a height around the base of the live branches, the magnitude of which is strongly influenced by the forest type and leaf area density. At this level, the turbulent wind-shearing stress may be depleted because momentum is absorbed most strongly through the upper canopy layers (i.e., within the tree crown [Shaw et al. 1974]). Therefore, equation (21) may be given instead as

$$0 = -\frac{\partial \overline{p}}{\partial x} - \frac{1}{2} C_d A \overline{U}^2 \ , \tag{25}$$

where wind speeds will tend to increase as the pressure drag forces decease across the trunk space in the absence of leaves and branches. It has been suggested that the low-level wind speed maximum in the lower portion of the forest canopy occurs in a transition layer between the upper canopy—extinction type profile and the log-law type wind speed profile that we would expect extends from this height to the ground.

3.4 1st-Order Closure and Higher-Order Closure Models of the Forest Canopy

Alternately, several authors have reported on the use of first-order closure models (Li et al. 1990; Wilson et al. 1998; Wilson and Flesch 1999; and Pinard and Wilson 2000) and higher-order closure models, to include large eddy simulations, to estimate wind speeds and turbulence within and above forest canopies (Wilson and Shaw 1977; Yamada 1982; Meyers and Paw U 1986; Meyers 1987; Wilson 1988; Paw U and Meyers 1989; Shaw and Schumann 1992; Shen and Leclerc 1997; Katul and Albertson 1998; Pyles et al, 2000; Albertson et al. 2001; and Li 2001). Primarily, the governing equations for these models, neglecting coriolis* and buoyancy forces, have been expressed

$$\frac{\partial \overline{u_j}}{\partial x_j} = 0 \ , \tag{26}$$

for continuity or conservation of matter, where $\overline{u}_j$ is the j-component of the vector $(\overline{u},\overline{v},\overline{w})$, and x_j is the j-component of the vector (x,y,z), and,

$$\frac{\partial \overline{u_i}}{\partial t} + \overline{u_j}\frac{\partial \overline{u_i}}{\partial x_j} + \frac{\partial \overline{u_i' u_j'}}{\partial x_j} = \frac{\partial \overline{p}}{\partial x_i} - \overline{\frac{\partial p'}{\partial x_i}} + \nu \frac{\partial^2 \overline{u_i}}{\partial^2 x_j} + \nu \overline{\frac{\partial^2 u_i'}{\partial^2 x_j}} \ , \tag{27}$$

for the mean flow (e.g., Wilson and Shaw 1977), where the overbar and primed variables indicate the mean and fluctuating components of the given quantity. Equation (27) contains the following terms from left to right: 1) time tendency of the mean wind, 2) advection of the mean wind, 3) eddy flux divergence, 4) the mean pressure gradient, 5) changes in the fluctuating component of static pressure (i.e., the pressure drag force), 6) the viscous drag accelerations on the mean flow, and 7) viscous drag accelerations on the canopy. The 5th and 7th terms represent "the summation of all the differential pressure forces (and velocity gradients) on the upstream and downstream sides of the elements of the (forest) canopy (Wilson and Shaw 1977)." Where pressure forces are considered the main portion of the total drag from the forest canopy, then the following closure assumption is made

---

*In meteorology, the coriolis force is an apparent (deflecting) force on moving air parcels in the atmosphere that arises due to the earth's rotation so that $f = -2\Omega \times V$, which is to the right of motion in the northern hemisphere (Huschke 1959). Here Ω is the angular velocity of the earth and V is velocity. Other than a few authors (e.g., Shinn 1971, Holland 1989, and Wilson and Flesch 1999), most exclude the effect of the coriolis force as having negligible effect on the scales of motion considered (i.e., windflow through the forest subcanopy layer see equation [25]).

$$\overline{\frac{\partial p'}{\partial x_i}} = C_d A \, \bar{u}_i^2 \ . \tag{28}$$

In addition, the most common first-order turbulence closure for the momentum flux divergence (term 3) in equation (27) can be expressed, as described by Li et al. (1990) as

$$\overline{\frac{\partial u_i' u_j'}{\partial x_j}} = \frac{\partial}{\partial x_j} K_{(ij)} \left(\frac{\partial \bar{u}_i}{\partial x_j} + \frac{\partial \bar{u}_j}{\partial x_i} \right) \tag{29}$$

where $K_{(ij)}$ is the viscosity (or eddy exchange coefficient) given by

$K_{(ij)} = l^2 \sqrt{\left(\frac{\partial \bar{u}_i}{\partial x_j}\right)^2 + \left(\frac{\partial \bar{u}_j}{\partial x_i}\right)^2}$, and l is a characteristic mixing length, which has been parameterized in various ways as a function of the forest height, canopy density, zero-plane displacement, and roughness (Li et al. 1990; Wilson et al. 1998; and Pinard and Wilson, 2001). Alternately, Wilson et al. (1998) specify the eddy exchange coefficient in terms of a characteristic mixing length scale, $\lambda_{mix} \propto l^{-1}$, and the square root of the turbulent kinetic energy, where $tke = \frac{1}{2}\sum u_i'^2$. As a result,

$$K = \lambda_{mix} \left(\frac{u_*^2}{tke(h)} tke(z) \right)^{\frac{1}{2}} \ , \tag{30}$$

where $\frac{u_*^2}{tke(h)}$ is the ratio of the equilibrium shearing stress and turbulent kinetic energy at the forest canopy top.

4. Vertical Profiles of Temperature in Forests

The forest canopy is an active surface for heat and moisture exchanges, and therefore, like over open fields, temperature profiles above the canopy top will form with inversions at night and unstable lapse rate conditions during the daytime (Munn 1966). However, temperature profiles above forests will not normally maintain large (positive or negative) gradients because of downward mixing (see discussion on wind speeds above the canopy top in section 3.2). Also, inversion conditions will sometimes develop during the daytime above forests due to evaporative cooling from leaf transpiration. In contrast, within the forest canopy, one mostly finds inversion conditions during the day and isothermal or slightly unstable lapse conditions at night (Figure 5). Bergen (1974) describes the diurnal variation of temperatures within the forest canopy in the following manner: a local temperature maximum develops between 0900 and 1000 LT, which moves downward into the canopy as solar altitude increases; the maximum penetration of heat is reached near 1200 LT at a height of about 0.7 h; variation in temperatures through the sub-

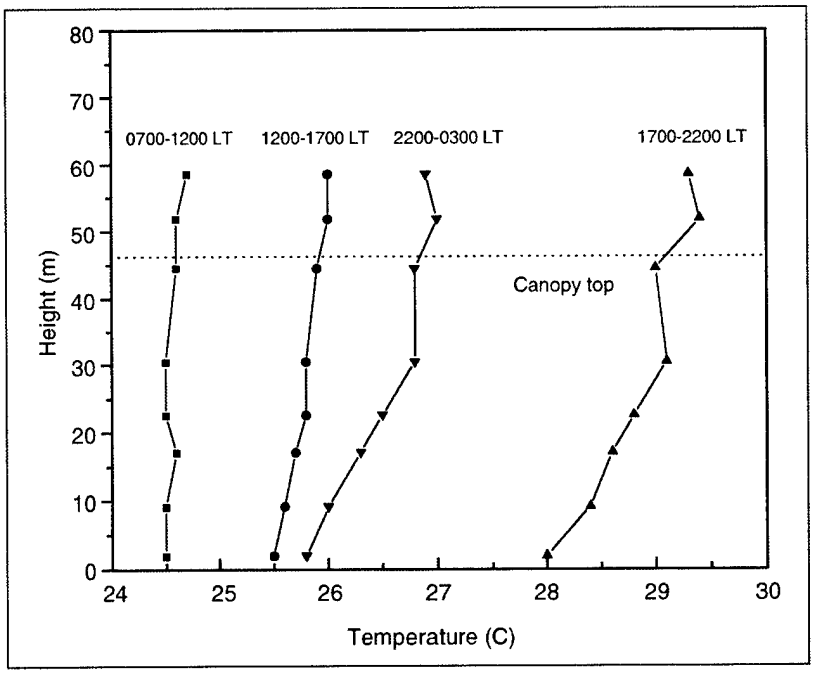

Figure 5. Observed mean temperatures (C) through a tropical rain forest canopy for different times of day (based on Bayton 1963).

canopy space is complex, but inversion conditions are often observed throughout the daytime period.

Likewise Raynor (1971) and Hosker et al. (1974) describe the forest canopy for heat absorption and radiative exchanges. During the daytime, the canopy captures incoming solar radiation and a layer of warm air develops that propagates downward through normal mixing processes. As an example, Figure 6 shows a typical, midday temperature profile for a pine forest stand on a clear day. Maximum temperatures are shown to coincide with the height of maximum leaf density (and minimum wind speeds; see Figure 2), whereas a local minimum in temperature occurs through the trunk space below the live branches. Under cloudy conditions with and without rainfall, Hosker et al. (1974) observed mostly isothermal conditions within a pine forest canopy throughout the day.

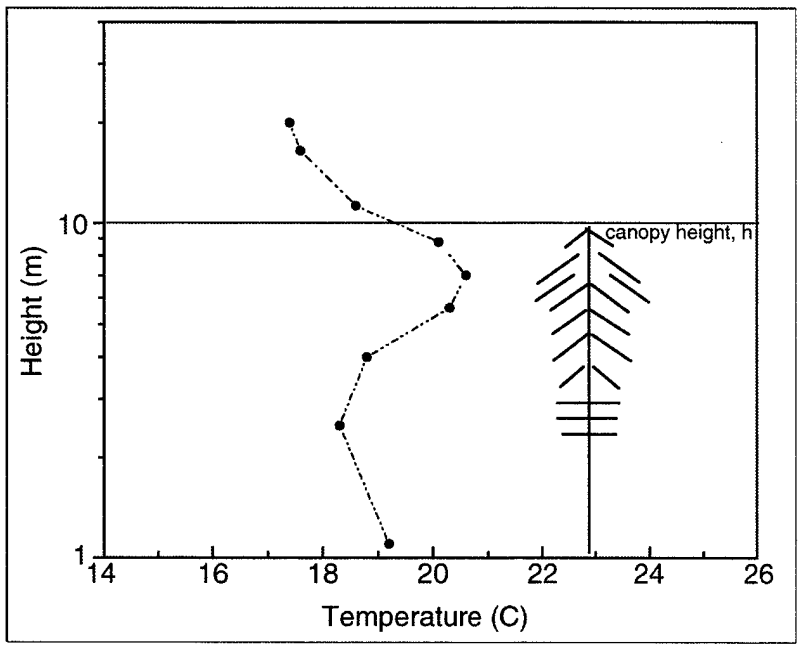

Figure 6. Typical vertical temperature profile structure within and above a pine forest stand (based on Bergen 1974).

In contrast at night, the forest canopy loses heat and is cooled further (from the upper crown area downward) by subsidence so that isothermal conditions or weak negative lapse rate conditions prevail. This was shown in the time sequence of vertical profiles reported by Huisman and Attenborough (1991). A second temperature inversion is likely to form close to the ground at night due to surface radiative cooling of the soil, as had been observed by Fontan et al. (1992) and Lee et al. (1997).

The conservation of energy (or enthalpy, $c_p\overline{\theta}$) equation can be written as described by Businger (1982) and Garratt (1992),

$$\frac{\partial\overline{\theta}}{\partial t} + \overline{u}_j\frac{\partial\overline{\theta}}{\partial x_j} = -\frac{\partial\left(\overline{u_j'\theta'}\right)}{\partial x_j} + \kappa_T\frac{\partial^2\overline{\theta}}{\partial x_j^2} + \frac{1}{\rho\, c_P}\frac{\partial\overline{R}_j}{\partial x_j} \tag{31}$$

where the terms from left to right are 1) the time tendency of the mean potential temperature ($\overline{\theta}$), 2) advection of potential temperature by the mean wind, 3) eddy heat flux divergence, 4) the viscous dissipation of heat and 5) the net radiative flux divergence through the forest canopy. The heat flux divergence term can be expanded as

$$\frac{\partial\left(\overline{u_j'\theta'}\right)}{\partial x_j} = \left(\frac{\partial\left(\overline{u'\theta'}\right)}{\partial x} + \frac{\partial\left(\overline{v'\theta'}\right)}{\partial y} + \frac{\partial\left(\overline{w'\theta'}\right)}{\partial z}\right). \tag{32}$$

Bergen (1974) suggested that

$$\frac{\partial\left(\overline{w'\theta'}\right)}{\partial z} \propto n\left(T_a - T_f\right) A \ , \tag{33}$$

where n is the heat transfer coefficient for the leaf (pine needle) surface, T_a is the air temperature, T_f is the leaf (needle) surface temperature, and A is the foliage surface area in the volume. Moreover, Bergen (1974) indicated that the value for (T_a–T_f) would depend on the solar altitude, the ratio of diffuse to direct solar radiation, and cloud cover. In addition, the angle between the wind velocity at the canopy top and the solar azimuth would be an important factor because of the influence (on temperature) from ventilation through opening at the canopy top and additional heating in direct sunlight. The reverse situation is considered for decreased wind flow and shaded areas in the lee of dense crowns. Intermittent wind gusts through openings at the top of the forest canopy are also important because they will bring downdrafts of cooler and drier air from above into the canopy (Denmead and Bradley 1985).

5. Acoustics in Forests

5.1 Approximation of Sound Speed Profiles in Forests

Figure 7 shows derived sound speed profiles within and above a 10 m (pine forest) canopy given the characteristic variations in wind speed and temperature that were described earlier in sections 3.1 and 4. Using equations (10–12) from section 1, the three plotted profiles represent from left to right 1) the effective sound speed, c_{eff}, along the path of propagation from the source to the receiver (i.e., upwind propagation [see Figure 1]), where $\theta_R = 90°$ is the bearing of the receiver from the source, and $\theta_w = 90°$ is the direction of the wind from North; 2) the speed of sound in air, c_0, from equation (10), which is the speed of sound in the absence of wind or crosswind propagation, and; 3) the effective sound speed, c_{eff}, where $\theta_R = 90°$ and $\theta_w = 270°$ (i.e., downwind propagation). The effective speed of sound for downwind propagation, $\theta_w = 270°$, is of a greater magnitude across the entire profile than in the opposite case (i.e., where $\theta_R = 90°$ and $q_w = 90°$). However, the sound speed profile here is flatter (and its slope above the canopy top is positive) in comparison to the other profiles. The influence these profile variations in sound speed have on short-range acoustic attenuation will be discussed briefly in the following section.

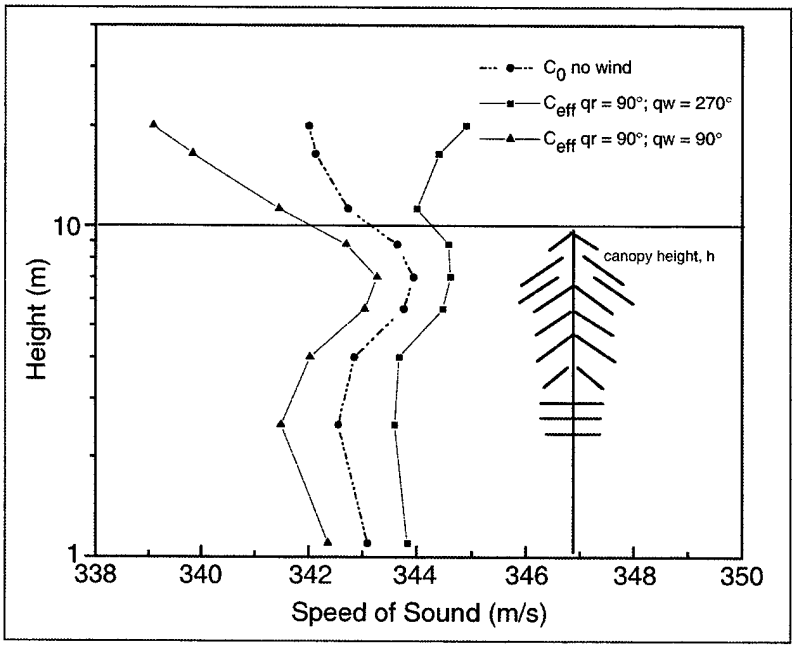

Figure 7. Derived speed of sound profiles within and above a 10-m pine forest canopy given the characteristic variations in wind speed and temperature that were shown in Figures (2) and (6). The three plotted profiles are described in the text.

5.2 Approximation of Short-Range Acoustic Attenuation in Forests

Attenuation of sound waves in forests is said to involve three main phenomena: 1) interference between direct and ground reflected acoustic waves; 2) scattering by tree trunks and branches, the ground, and turbulence; and 3) absorption by the trees, leaves, branches, the ground, and the air (Erying 1946; Embleton 1963; Aylor 1972; Burns 1979; Fricke 1984; Attenborough 1985; Price et al. 1988; Huismann and Attenborough 1991; and Sakai et al. 1998, 2001). Ground impedance, which affects sound-wave reflection and absorption, has been found to be a function of flow resistivity and ground surface porosity. Ground impedance has been reported to affect sound attenuation mainly in the 250–500 Hz frequency range (Fricke 1984; Price et al. 1988; and Sakai et al. 2001). Flow resistivities for ground surfaces under typical forest stands have been reported as σ = 20–80 kPa s m^{-2}, which are much lower in comparison to those reported for grass (σ = 150–300 kPa s m^{-2}) or soil covered surfaces (σ = 300–800 kPa s m^{-2}) (Embleton et al., 1983). Likewise, the forest floor, which consists of humus, leaves (needles), and other biological litter, has been reported to have values for porosity of about Ω = 0.825, which are considerably higher than those reported for grass fields (Ω = 0.675) or unpacked soils (Ω = 0.575) (Attenborough 1985).

At higher frequencies ($f \geq$ 1 to 2 kHz), sound attenuation in forests has been observed as being mainly due to scattering by tree trunks and branches and absorption by foliage (Embleton 1963; Aylor 1972; Burns 1979; Fricke 1984; Price et al. 1988; and Huismann and Attenborough 1991). These effects on sound attenuation at higher frequencies may be as important as refraction

effects due to temperature inversions and wind speeds within the forest canopy (Huismann and Attenborough 1991).

To provide an example, we have used the characteristic profiles of wind speed and temperature, which were shown in Figures (2) and (6) as input to a flat-earth, nonturbulent, acoustic propagation model called WSCAFFIP (the Windows (version) Scanning Fast Field Program). WSCAFFIP is a numerical code developed for assessing environmental effects on short-range acoustic attenuation (Noble and Marlin 1995). WSCAFFIP determines acoustic attenuation as relative sound pressure loss with range and azimuth for a given frequency and source–receiver geometry. WSCAFFIP contains propagation algorithms to represent the effects of atmospheric refraction, diffraction, absorption, and reflection (ground impedance) on acoustic transmission. Table 2 lists the model parameters for an initial approximation of short-range acoustic attenuation in forests. The distance of the receiver from the source, source height, and receiver height were 500 m, 2 m, and 1 m, respectively. We have calculated relative attenuation at 50, 100, 500, and 1000 Hz for upwind propagation ($\theta_R = 90°$ and $\theta_w = 90°$) and downwind propagation ($\theta_R = 90°$ and $\theta_w = 270°$). Figure 8 shows the WSCAFFIP results for the sound speed profiles described in section 5.1.

Table 2. WSCAFFIP model parameters for approximation of short-range acoustic attenuation in forests.

Parameter	Symbol	Value
Distance of receiver from source	x	500 m
Range resolution	Δx	10 m
Bearing of receiver from source	θ_R	90°
Source height above ground	h_S	2 m
Receiver height above ground	h_R	1 m
Frequency of interest	f	50 Hz; 100 Hz, 500 Hz; 1000 Hz
Ground porosity	Ω	0.850
Flow resisitivity	σ	23 kPa s m^{-2}
Bearing of the wind from North	θ_w	90° ; 270°

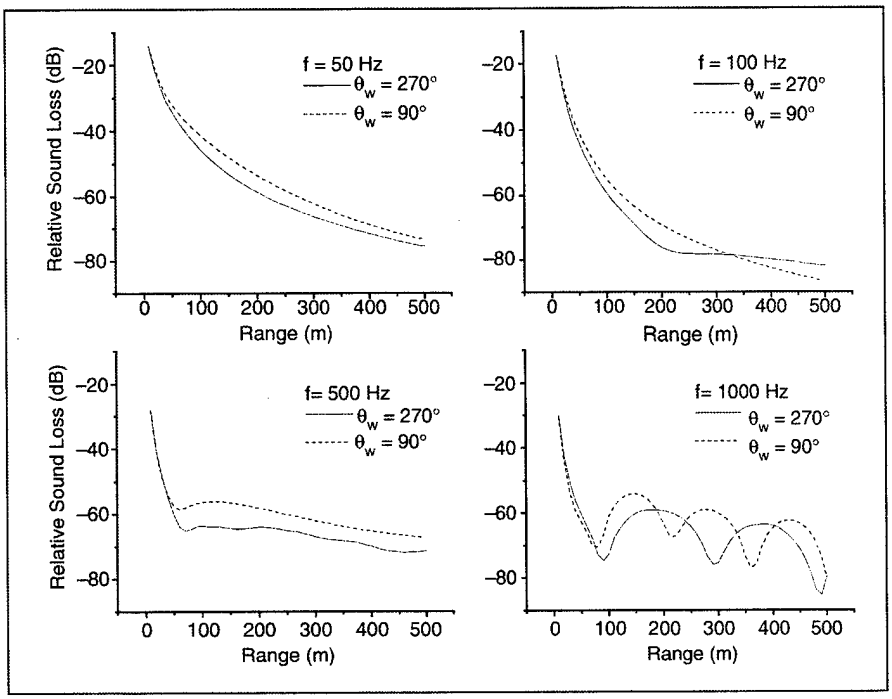

Figure 8. WSCAFFIP numerical approximations of short-range acoustic attenuation within a continuous forest stand. Calculations of relative attenuation are shown at 50, 100, 500, and 1000 Hz for $\theta_R = 90°$ and $\theta_w = 90°$ and 270°.

Acoustic waves within and above the forest canopy will tend to be refracted upward as the effective sound speed decreases with height and refracted downward as sound speed increases with height. Therefore, we might expect the amounts of attenuation to depend on the strength and locations of sound speed profile inversions between the ground and the forest canopy top. Because the sound speed profile for $\theta_w = 270°$ was comparatively flatter than that for $\theta_w = 90°$ we would expect to see slightly greater attenuation with range for $\theta_w = 270°$ at each frequency as a result. Figure 8 shows this result satisfactorily, even though ground impedance, more that sound speed profile shape, may have affected the model results at frequencies $\leq$ 500 Hz (Embleton 1996).

Finally, in preparing this report for publication a reviewer offered the following comments: The behavior of the results shown in Figure 8 can be roughly understood in terms of 'ducting' of acoustic modes. An acoustic duct exists between the surface and about 7 m. At lower frequencies, 50 and 100 Hz, acoustic waves may be too long for any significant ducting to occur. At 500 Hz, there appears to be a single trapped mode; while at 1000 Hz, it appears that two modes are trapped, creating the interference pattern (Wilson 2002). Thus, it is the 'ducting' of acoustic modes inside and above the forest canopy that is greatly influenced by variations in local wind speed and temperature profile structure.

6. Summary and Conclusions

We have initiated research to examine the calculation of local speed of sound in the forest environment for future military applications of acoustic information in forests. We gathered information from the literature on measured and modeled micrometeorology in forests to include reports on wind speed and temperature profile structure, turbulence, leaf area distributions, and estimates of surface roughness and displacement. (An Appendix summarizes the results of the literature survey from which the report was produced.) We also derived initial approximations for sound speed and short-range acoustic attenuation through a continuous forest stand based on two characteristic profiles for wind speed and temperature inside and above the forest canopy.

As discussed in section 5.2, attenuation of sound waves in forests is affected by interference between direct and ground reflected acoustic waves, refraction, scattering, and absorption. Because acoustic waves tend to be refracted upward as the effective sound speed decreases with height and refracted downward as sound speed increases with height, we expect that attenuation will depend greatly on the strength and locations of sound speed profile inversions between the ground and the forest canopy top. Several initial model calculations showed this result satisfactorily. We expect that the information gathered as a result of this survey will be useful to help evaluate various meteorological computer models and techniques for determining vertical profiles of sound speed through the atmosphere in forests.

References

Albertson, J. D., G. G. Katul, and P. Wiberg. "Relative Importance of Local and Regional Controls on Coupled Water, Carbon, and Energy Fluxes." *Advances in Water Resources*, vol. 24, pp. 1103–1118, 2001.

Albini, F. A. "A Phenomenological Model for Wind Speed and Shear Stress Profiles in Vegetation Cover Layer." *Journal of Applied Meteorology*, vol. 20, pp. 1325–1335, 1981.

Allen, L. H., Jr. "Turbulence and Wind Speed Spectra Within a Japanese Larch Plantation." *Journal of Applied Meteorology*, vol. 7, pp. 73–78, 1968.

Amiro, B. D., and P. A. Davis. "Statistics of Atmospheric Turbulence Within a Natural Black Spruce Forest Canopy." *Boundary Layer Meteorology*, vol. 44, pp. 267–283, 1988.

Arya, S. P. *Introduction to Micrometeorology*. Second Edition, p. 420, San Diego: Academic Press, 2001.

Attenborough, K. "Acoustical Impedance Models for Outdoor Surfaces." *Journal of Sound Vibration*, vol. 99, pp. 521–544, 1985.

Auvermann, H. J., and G. H. Goedecke. "Acoustic Scattering into Shadow Zones From Atmospheric Turbulence." Presented at the Fourth Annual Ground Target Modeling & Validation Conference, Houghton, MI, August 1993.

Auvermann, H. J., R. L Reynolds, and D. M. Brown. "Development of a Multistream Acoustic Propagation Model Including Scattering by Turbulence." ARL-TR-528, U.S. Army Research Laboratory, Adelphi, MD, 1995.

Auvermann, H. J. "Turbule Ensemble Model of Atmospheric Turbulence: Progress in its Development and Use in Acoustical-Scattering Investigations." ARL-SR-101, U.S. Army Research Laboratory, Adelphi, MD, 2001.

Aylor, D. "Noise Reduction by Vegetation and the Ground." *Journal of the Acoustical Society of America.*, vol. 51, pp. 197–205, 1972.

Baldocchi, D. D., and B. A. Hutchinson. "Turbulence in an Almond Orchard: Spatial Variations in Spectra and Coherence." *Boundary Layer Meteorology*, vol. 42, pp. 293–311, 1988.

Baldocchi, D. D., and T. P. Meyers. "Turbulence Structure in a Deciduous Forest." *Boundary Layer Meteorology*, vol. 43, pp. 345–364, 1988.

Barr, S. "A Modeling Study of Several Aspects of Canopy Flow." *Monthly Weather Review*, vol. 99, pp. 485–493, 1971.

Bayton, H. W. "The Penetration and Diffusion of a Fine Aerosol in a Tropical Rain Forest." Ph.D. Thesis, pp. 118–209, Univ. of Michigan, Ann Arbor, MI, 1963.

Becker, G., and A. Güdesen. "Passive Sensing with Acoustics on the Battlefield." *Applied Acoustics*, vol. 59, pp. 149–178, 2000.

Benn, B. O., and G. H. Hilt. "Rationale and Plan for Field Data Acquisition Required for the Rational Design and Evaluation of Seismic and Acoustic Classifying Sensors." WES-MP-M-75-10, U.S. Army Engineer Waterways Experiment Station, Vicksburg, MS, 1975.

Benoit, R. "On the Integral of the Surface Layer Profile-Gradient Functions." *Journal of Applied Meteorology*, vol. 16, pp. 859–860, 1977.

Bergen, J. D. "Vertical Profiles of Windspeed in a Pine Stand." *Forest Science*, vol. 17, pp. 314–322, 1971.

Bergen, J. D. "Vertical Air Temperature Profiles in a Pine Stand: Spatial Variation and Scaling Problems." *Forest Science*, vol. 20, pp. 64–73, 1974.

Burns, S. H. "The Absorption of Sound by Pine Trees." *Journal of the Acoustical Society of America*, vol. 65, pp. 658–661, 1979.

Busch, N. E. "On the Mechanics of Atmospheric Turbulence." in *Workshop on Micrometeorology*, D. A. Haugen, (ed.), American Meteorological Society, pp. 1–65, Boston, MA, 1973.

Businger, J. A. "Equations and Concepts." in *Atmospheric Turbulence and Air Pollution Modeling*, pp. 1–36, F.T.M. Nieuwstadt and H. van Dop (eds.), Dordrecht, The Netherlands: D. Reidel Publishing, 1982.

Carnes, B. L., and J. C. Morgan. "Evaluation of the Sensitivity and Limits of the Passive Acoustic Ranging Algorithm for Single and Multiple Helicopters." WES/TR/SL-95-8, U.S. Army Engineer Waterways Experiment Station, Structures Laboratory, Vicksburg, MS, 1995.

Chen, J. M., T. A. Black, M. D. Novak, and R. S. Adams. "A Wind Tunnel Study of Turbulent Airflow in Forest Clearcuts" *in Wind and Trees*. pp. 71–87, M. P. Coutts and J. Grace (eds.), England: Cambridge University Press, 1995.

Cionco, R. M. "A Mathematical Model for Air Flow in a Vegetative Canopy." *Journal of Applied Meteorology*, vol. 4, pp. 517–522, 1965.

Coutts, M. P., and J. Grace (eds.). *Wind and Trees*. England: Cambridge University Press, 1995.

Depireux, D. A., and S. A. Shamma. "Vehicle Classification Using a Biological Model of Hearing." N00014-97-1-0501, University of Maryland, College Park, Inst. for Systems Research, College Park, MD, 2000.

DeMarrais, G. A. "Wind Speed Profiles at Brookhaven National Laboratory." *Journal of Meteorology*, vol. 16, pp. 181–190, 1959.

Denmead, O. T., and E. F. Bradley. "Flux-Gradient Relationships in a Forest Canopy. *The Forest-Atmosphere Interaction*, pp. 421–442, B. A. Hutchinson and B. B. Hicks, (eds.), Dordrecht, The Netherlands: D. Reidel Publishing Co., Dordrecht, The Netherlands, 1985.

Dyer, A. J. "A Review of Flux-Profile Relationships." *Boundary Layer Meteorology.*, vol. 1, pp. 363–372, 1974.

Embleton, T. F. W. "Sound Propagation in Homogeneous Deciduous and Evergreen Woods." *Journal of the Acoustical Society of America.*, vol. 35, pp. 1119–1125, 1963.

Embleton, T. F. W. "Tutorial on Sound Propagation Outdoors." *Journal of the Acoustical Society of America.*, vol. 100, pp. 31–48, 1996.

Embleton, T. F. W., J. E. Piercy, and G. A. Daigle. "Effective Flow Resistivity of Ground Surfaces Determined by Acoustical Measurements." *Journal of the Acoustical Society of America.*, vol. 74, pp. 1239–1244, 1983.

Eom, K., M. Wellman, N. Srour, D. Hillis, and R. Chellappa. "Acoustic Target Classification Using Multiscale Methods." DTIC Internet Document, U.S. Army Research Laboratory, Adelphi, MD, 1999.

Erying, C. F. "Jungle Acoustics." *Journal of the Acoustical Society of America.*, vol. 18, pp. 257–270, 1946.

Finnigan, J. J., and Y. Brunet. "Turbulent Air Flow in Forests on Flat and Hilly Terrain" *in Wind and Trees*. pp. 3–39, M. P. Coutts, and J. Grace (eds.), England: Cambridge University Press, 1995.

Fleagle, R. G., and J. A. Businger. *An Introduction to Atmospheric Physics*. p. 346, New York: Academic Press, 1963.

Fong, M., and N. Srour. "Cueing of the Surrogate Remote Sentry Using an Acoustic Detection System." ARL-TR-795, U.S. Army Research Laboratory, Adelphi, MD, 1994.

Fontan, J., A. Minga, A. Lopez, and A. Druilhet. "Vertical Ozone Profiles in a Pine Forest." *Atmospheric Environment*, vol. 26A, pp. 863–869, 1992.

Fricke, F. "Sound Attenuation in Forests." *Journal of Sound and Vibration*, vol. 92, pp. 149–158, 1984.

Garratt, J. R. "Surface Influence Upon Vertical Profiles in the Atmospheric Near-Surface Layer." *Quarterly Journal of the Royal Meteorological Society.*, vol. 106, pp. 803–819, 1980.

Garratt, J. R. *The Atmospheric Boundary Layer*. United Kingdom: Cambridge University Press, p. 316, 1992.

Goedecke, G. H., M. DeAntonio, and H. J. Auvermann. "First-Order Acoustic Wave Equations and Scattering by Atmospheric Turbules." ARL-TR-1356, U.S. Army Research Laboratory, Adelphi, MD, 1977.

Goedecke, G. H., R. C. Wood, and H. J. Auvermann. "Doppler Broadening of Acoustic Waves Scattered by Turbulence Flowing With a Horizontal Wind." ARL-TR-2131, U.S. Army Research Laboratory, Adelphi, MD, 2000.

Hafner, E., S. Schodowski, J. R. Vig, and H. Mazurczyk. "Gunhardened Crystal Oscillators for Remotely Monitored Battlefield Sensor System." ECOM-4441, U.S. Army Electronics Command, Fort Monmouth, NJ, 1976.

Holland, J. Z. "On Pressure-Driven Wind in Deep Forests." *Journal of Applied Meteorology*, vol. 28, pp. 1349–1355, 1989.

Hosker, R. P., Jr., C. J. Nappo, and S. R. Hanna. "Diurnal Variation of Vertical Thermal Structure in a Pine Plantation. *Agricultural Meteorology.*, vol. 13, pp. 259–265, 1974.

Huismann, W. H. T., and K. Attenborough. "Reverberation and Attenuation in a Pine Forest." *Journal of the Acoustical Society of America.*, vol. 90, pp. 2664–2677, 1991.

Huschke, R. E. (ed.). *Glossary of Meteorology*, pp. 638, American Meteorological Society, Boston, MA, 1959.

Inoue, E., "On the Turbulent Structure of Airflow Within Crop Canopies." *Journal of the Meteorological Society of Japan*, vol. 41, pp. 317–326, 1963.

Irwin, J. S. "A Theoretical Variation of the Wind Profile Power-Law Exponent as a Function of Surface Roughness and Stability." *Atmospheric Environment*, vol. 13, pp. 191–194, 1979.

Jacobs, A. F. G., J. H. van Boxel, and R. M. M. El-Kilani. "Vertical and Horizontal Distribution of Wind Speed and Air Temperature in a Dense Vegetation Canopy." *Journal of Hydrology*, vol. 166, pp. 313–326, 1995.

Kaimal, J. C., and J. J. Finnegan. *Atmospheric Boundary Layer Flows: Their Structure and Measurement.* p. 289, New York: Oxford University Press, 1994.

Katul, G. G., and J. D. Albertson. "An Investigation of Higher-Order Closure Models for a Forested Canopy." *Boundary Layer Meteorology,* vol. 89, pp. 47–74, 1998.

Kotiaho, M. P. "Improvements to the Acoustic Multistream Propagation Program." ARL-CR-209, U.S. Army Research Laboratory, Adelphi, MD, 1996.

Lee, X. ,and A. Black. "Atmospheric Turbulence Within and Above a Douglas-Fir Stand. Part I: Statistical Properties of the Velocity Field." *Boundary Layer Meteorology*, vol. 64, pp. 149–174, 1993.

Lee, X., H. H. Neumann, G. den Hartog, J. D. Fuentes, T. A. Black, R. E. Mickle, P. C. Yang, and P. D. Blanken. "Observations of Gravity Waves in a Boreal Forest." *Boundary Layer Meteorology*, vol. 84, pp. 383–398, 1997.

Li, J. C. "Large Eddy Simulation of Complex Turbulent Flows: Physical Aspects and Research Trends." *Acta Mechanica Sinica (English Series)*, vol. 17, pp. 289–301, 2001.

Li, Z., J. D. Lin, and D. R. Miller. "Air Flow Over and Through a Forest Edge: A Steady-State Numerical Simulation." *Boundary Layer Meteorology*, vol. 51, pp. 179–197, 1990.

Lo, A. K. "Determination of Zero-Plane Displacement and Roughness Height of a Forest Canopy Using Profiles of Limited Height." *Boundary Layer Meteorology*, vol. 75, pp. 381–402, 1995.

Lopez, J. E., J. C . Lo, and J. Saulnier. "Vehicle Signal Enhancement Using Packet Wavelet Transform and Nonlinear Noise Processing Techniques." SBIR Contract No. DAAE30-98-C-1067, Cytel Systems Inc., Hudson, MA, 1999.

Martin, H. C. "Average Winds Above and Within a Forest." *Journal of Applied Meteorology*, vol. 10, pp. 1132–1137, 1971.

Massman, W. J. "Foilage Distribution in Old-Growth Coniferous Tree Canopies." *Canadian Journal of Forest Research*, vol. 12, pp. 10–17, 1982.

Mays, B. T., and J. Price. "A Multi-Tier Cluster Based Tracker Approach for Battlefield Acoustic Systems." DTIC Internet Document, U.S. Army Research Laboratory, Adelphi, MD, 2000.

Mays, B. T., and H. Q. Vu. "Data Fusion and Tracking System Testbed." DTIC Internet Document, U.S. Army Research Laboratory, Adelphi, MD, 2000.

Meroney, R. N. "Characteristics of Wind and Turbulence in and Above Model Forests." *Journal of Applied Meteorology*, vol. 7, pp. 780–788, 1968.

Meyers, T. P., and K. T. Paw U. "Testing of a Higher Order Closure Model for Modeling Airflow Within and Above Plant Canopies." *Boundary Layer Meteorology*, vol. 37, pp. 297–311, 1986.

Meyers, T. P. "The Sensitivity of Modeled SO_2 Fluxes and Profiles to Stomatal and Boundary Layer Resistances." *Water Air and Soil Pollution*, vol. 35, pp. 261–278, 1987.

Meyers, T. P., P. Finkelstein, J. Clarke, T. G. Ellestad, and P.F. Sims. "A Multilayer Model for Inferring Dry Deposition Using Standard Meteorological Measurements." *Journal of Geophysical Research*, vol. 103, pp. 22,645–22,661, 1998.

Miller, D. R., Y. Wang, K. Ducharne, M. A. McManus, R. Reardon, W. Yendol, K. Meirzjewski. "Wind and Stability Effects on Aerial Spray Penetration Into a Hardwood Forest." in Proceedings of the 21st Conference of Agricultural and Forest Meteorology, 7–11 March, San Diego, CA, American Meteorological Society, Boston, MA, 1994.

Monin, A. S., and A. M. Obukhov. "Basic Regularity in Turbulent Mixing in the Surface Layer of the Atmosphere." *Trudy, Akademiia Nauk S.S.S.R., Geofizicheskogo Instituta*, vol. 24, p. 151, 1954.

Munn, R.E. *Descriptive Micrometeorology*. p. 245, New York: Academic Press, 1966.

Noble, J. M. "Evaluation of Simple Spherical Spreading Model for Near Vertical Acoustical Propagation." ARL-TR-532, U.S. Army Research Laboratory, Adelphi, MD, 1994.

Noble, J. M., and D. Marlin. "User's Manual for the Scanning Fast Field Program (SCAFFIP) General Version 1.0." ARL-TR-545, U.S. Army Research Laboratory, Adelphi, MD, 1995.

Oke, T. R. *Boundary Layer Climates*, London Methuen, p. 372, 1978.

Oliver, H. R. "Wind Profiles in and Above a Forest Canopy." *Quarterly Journal of the Royal Meteorological Society*, vol. 97, pp. 548–553, 1971.

Osteshev, V. E. "Acoustics in Moving Inhomogeneous Media." *E&FN Spon, London*, vol. 16, no. 67, pp. 193–218, 1997.

Panofsky, H. A. "Determination of Stress from Wind and Temperature Measurements." *Quarterly Journal of the Royal Meteorological Society*, vol. 89, pp. 85–94, 1963.

Paulson, C. A. "The Mathematical Representation of Wind Speed and Temperature Profiles in the Unstable Atmospheric Surface Layer." *Journal of Applied Meteorology*, vol. 9, pp. 57–61, 1970.

Paw U, K. T., and T. P. Meyers. "Investigations with a Higher-Order Canopy Turbulence Model into Mean Source-Sink Levels and Bulk Canopy Resistances." *Agricultural and Forest Meteorology*, vol. 47, pp. 259–271, 1989.

Pielke, R. A. *Mesoscale Meteorological Modeling.* New York: Academic Press, p. 612, 1984.

Pilette, S., B. Biggs, and H. Martinek. "Requirements for Target Identification Training for the Acoustic Sensor Operator." Contract No. DAHC19-76-C-0034, HRB-Singer Inc., State College, PA, 1979.

Pinard, J. D. J.-P., and J. D. Wilson. "First- and Second-Order Closure Models for Wind in a Plant Canopy." *Journal of Applied Meteorology*, vol. 40, pp. 1762–1768, 2001.

Price, M. A., K. Attenborough, and N. W. Heap. "Sound Attenuation Through Trees: Measurements and Models." *Journal of the Acoustical Society of America.*, vol. 84, pp. 1836–1844, 1988.

Pyles, R. D., B. C. Weare, and K. T. Paw U. "The UCD Advanced Canopy-Atmosphere-Soil Algorithm: Comparisons with Observations From Different Climate and Vegetation Regimes." *Quarterly Journal of the Royal Meteorological Society*, vol. 126, pp. 2951–2980, 2000.

Rachele, H., and A. Tunick. "Energy Balance Model for Imagery and Electromagnetic Propagation." *Journal of Applied Meteorology*, vol. 33, pp. 964–976, 1994.

Raynor, G. S. "Wind and Temperature Structure in a Coniferous Forest and Contiguous Field." *Forest Science*, vol. 17, pp. 351–363, 1971.

Raynor, G. S., J. V. Hayes, and E. C. Ogden. "Particulate Dispersion Into and Within a Forest." *Boundary Layer Meteorology*, vol. 7, pp. 429–456, 1974.

Raynor, G. S., J. V. Hayes, and E. C. Ogden. "Particulate Dispersion Form Sources Within a Forest." *Boundary Layer Meteorology*, vol. 9, pp. 257–277, 1975.

Rosenthal, F., and J. C. Stevens. "Passive Aero-Acoustic Sensor Self Interference Cancellation." Phase 1. Contract No. DAAA21-94-C-0025, Signal Separation Technologies, Annandale, VA, 1994.

Sadeh, W. Z., J. E. Cermak, and T. Kawatani. "Flow Over High Roughness Elements." *Boundary Layer Meteorology*, vol. 1, pp. 321–344, 1971.

Sakai, H., S. Shibata, and Y. Ando. "Orthogonal Acoustical Factors of Sound Fields in a Forest Compared with Those in a Concert Hall." *Journal of the Acoustical Society of America.*, vol. 104, pp. 1491–1497, 1998.

Sakai, H., S. Sato, and Y. Ando. "Orthogonal Acoustical Factors of a Sound Fields in a Bamboo Forest. *Journal of the Acoustical Society of America.*, vol. 109, pp. 2824–2830, 2001.

Shaw, R. H. "Secondary Wind Speed Maxima Inside Plant Canopies." *Journal of Applied Meteorology*, vol. 16, pp. 514–521, 1977.

Shaw, R. H., R. H. Silversides, and G. W. Thurtell. "Some Observations of Turbulence and Turbulent Transport Within and Above Plant Canopies." *Boundary Layer Meteorology*, vol. 5, pp. 429–449, 1974.

Shaw, R. H., and A. R. Periera. "Aerodynamic Roughness of a Plant Canopy: A Numerical Experiment." *Agricultural Meteorology*, vol. 26, pp. 51–65, 1982.

Shaw, R. H., G. den Hartog, and H. H. Neumann. "Influence of Foliar Density and Thermal Stability on Profiles of Reynolds Stress and Turbulence Intensity in a Deciduous Forest." *Boundary Layer Meteorology*, vol. 45, pp. 391–409, 1988.

Shaw, R. H., and U. Schumann. "Large-Eddy Simulation of Turbulent Flow Above and Within a Forest." *Boundary Layer Meteorology*, vol. 61, pp. 47–64, 1992.

Shen, S. H., and M. Y. Leclerc. "Modelling the Turbulence Structure in the Canopy Layer." *Agricultural Forest Meteorology,* vol. 87, pp. 3–25, 1997.

Shinn, J. H. "Steady-State Two-Dimensional Air Flow in Forests and the Disturbance of Surface Layer Flow by a Forest Wall." ECOM-5383, U.S. Army Electronics Command, Fort Monmouth, NJ, p. 86, 1971.

Smith, G. E. "Focusing on Acoustic Waves in a Non-Uniform Atmosphere." MRL-TR-89-10, Material Technology Laboratory, U.S. Army Laboratory Command, Watertown, MA, 1989.

Sparrow, V. W. "A Finite Difference Numerical Model for the Propagation of Finite Amplitude Acoustical Blast Waves Outdoors Over Hard and Porous Surfaces." CERL-TM-N-91/23, U.S. Army Construction Engineering Research Laboratory, Champaign, IL, 1991.

Srour, N., and J. Robertson. "Remote Netted Acoustic Detection System: Final Report. ARL-TR-706, U.S. Army Research Laboratory, Adelphi, MD, 1995.

Thompson, A. A., and C. K. Scherer. "Direction and Location of Artillery Rockets by Acoustic Techniques." BRL-TR-3231, U.S. Army Ballistic Research Laboratory, Aberdeen Proving Ground, MD, 1991.

Touma, J. S. "Dependence of the Wind Profile Power Law on Stability for Various Locations." *Journal of the Air Pollution Control Association*, vol. 27, pp. 863–866, 1977.

Webb, W. K. "Profile Relationships: The Log-Linear Range, and Extension to Strong Stability." *Quarterly Journal of the Royal Meteorological Society*, vol. 96, pp. 67–90, 1970.

Wellman, M. "Performance of Classifier Architectures With the RNADS Feature Space." DTIC Internet Document, U.S. Army Research Laboratory, Adelphi, MD, 1999.

Wellman, M, and N. Srour. "Enhanced Target Identification Using Higher Order Shape Statistics." ARL-TR-1723, U.S. Army Research Laboratory, Adelphi, MD, 1999.

West, M., R. A. Sack, and F. Walkden. "The Fast Field Program (FFP). A Second Tutorial: Application to Long Range Sound Propagation in the Atmosphere." *Applied Acoustics*, vol. 33, pp. 199–228, 1991.

West, M., K. Gilbert, and R. A. Sack. "A Tutorial on the Parabolic Equation (PE) Model Used for Long Range Sound Propagation in the Atmosphere." *Applied Acoustics*, vol. 37, pp. 31–49, 1992.

Wilson, D. K. Personal communication, U.S. Army Research Laboratory, Adelphi, MD, 2002.

Wilson, D. K. "Sound Field Computations in a Stratified, Moving Medium." *Journal of the Acoustical Society of America.*, vol. 94, pp. 400–407, 1993.

Wilson, D. K. "Performance of Acoustic Tracking Arrays in Atmospheric Turbulence." ARL-TR-1286, U.S. Army Research Laboratory, Adelphi, MD, 1997.

Wilson, D. K. "A Prototype Acoustic Battlefield Decision Aid Incorporating Atmospheric Effects and Arbitrary Sensor Layouts." ARL-TR-1708, U.S. Army Research Laboratory, Adelphi, MD, 1998a.

Wilson, D. K. "Anisotropic Turbulence Models for Acoustic Propagation Through the Neutral Atmospheric Surface Layer." ARL-TR-1519, U.S. Army Research Laboratory, Adelphi, MD, 1998b.

Wilson, D. K. "A Turbulence Spectral Model for Sound Propagation in the Atmosphere That Incorporates Shear and Buoyancy Forcings." *Journal of the Acoustical Society of America*, vol. 108, pp. 2021–2038, 2000.

Wilson, D. K., and G. L. Szeto. "Reference Guide for the Acoustic Battlefield Aid (ABFA) Version 2." ARL-TR-2159, U.S. Army Research Laboratory, Adelphi, MD, 2000.

Wilson, D. K., G. L. Szeto, B. H. Van Aartsen, and J. M. Noble. "A Prototype Acoustic Battlefield Decision Aid with Interfaces to Meteorological Data Sources and a Target Database." DTIC Internet Document, U.S. Army Research Laboratory, Adelphi, MD, 2000.

Wilson, J. D. "A Second-Order Closure Model for Flow Through Vegetation." *Boundary Layer Meteorology*, vol. 42, pp. 371–392, 1988.

Wilson, J. D., J. J. Finnegan, and M. R. Raupach. "A First-Order Closure for Disturbed Plant-Canopy Flows, and its Application to Winds in a Canopy on a Ridge." *Quarterly Journal of the Royal Meteorological Society*, vol. 124, pp. 705–732, 1998.

Wilson, J. D., and T. K. Flesch. "Wind and Remnant Tree Way in Forest Cutblocks. III. A Windflow Model to Diagnose Spatial Variation." *Agricultural Forest Meteorology*, vol. 93, pp. 259–282, 1999.

Wilson, N. R., and R. H. Shaw. "A Higher Order Model for Canopy Flow." *Journal of Applied Meteorology*, vol. 16, pp. 1197–1205, 1977.

Wong, G. S. K. "Speed of Sound in Standard Air." *Journal of the Acoustical Society of America*, vol. 79, pp. 1359–1366, 1986.

Wong, G. S. K., and T. F. W. Embleton. "Variation of Specific Heats and of Specific Heat Ratio in Air with Humidity." *Journal of the Acoustical Society of America.*, vol. 76, pp. 555–559, 1985.

Wong, G. S. K., and T. F. W. Embleton. "Variation of the Speed of Sound in Air With Humidity and Temperature." *Journal of the Acoustical Society of America*, vol. 77, pp. 1710–1712, 1984.

Yamada, T. "A Numerical Model Study of Turbulent Airflow In and Above a Forest Canopy." *Journal of the Meteorological Society of Japan*, vol. 60, pp. 439–454, 1982.

Young, S., P. Budulas, P. Emmerman, M. Scanlon, N. Srour, D. Hillis, P. David, P. Fisher, S. Vinci, A. Harrison, K. Gurton, S. Crow, and M. Wellman. "RSTA for Small Rovers in Urban Warfare." ARL-TR-1678, U.S. Army Research Laboratory, Adelphi, MD, 1999.

Zappi, M. A. "Status Report for Selection of Sites for Background Noise Signature Data Base Development." WES-MP-M-78-1, U.S. Army Engineer Waterways Experiment Station, Vicksburg, MS, 1978.

Zoumakis, N. M. "Estimating the Zero-Plane Displacement and Roughness Length for Tall Vegetation and Forest Canopies Using Semi-Empirical Wind Profiles." *Journal of Applied Meteorology*, vol. 32, pp. 574–579, 1993.

Zoumakis, N. M. "Determination of the Mean Wind Speed and Momentum Diffusivity Profiles Above Tall Vegetation and Forest Canopies Using a Mass Conservation Assumption." *Journal of Applied Meteorology*, vol. 33, pp. 295–303, 1994.

Appendix – Literature Survey

This Appendix contains several tables to list the numerous citations associated with the topics discussed in the report, i.e.,

- Battlefield acoustic models and acoustic sensor arrays,
- Speed of sound physics,
- Observed micrometeorology in forests,
- Computer models to provide meteorological profile and turbulence information within and above forests,
- Forest characteristics to include leaf area density, roughness, and displacement height, and
- Measurements and approximations of short-range acoustic attenuation in forests.

Table A-1. The Future Combat System's battlefield.

U.S. Army Acoustic Systems: a. Surveillance, b. Tracking, c. Detection, d. Identification, e. Classification, f. Remote sentry, and g. Intelligence gathering of military targets. New U.S. Army acoustic systems include unattended ground sensors (UGS) in remote netted acoustic/seismic sensor arrays (RNADS).	Benn and Hilt (1975); Hafner et al. (1976); Zappi (1978); Pilette et al. (1979); Thompson and Scherer (1991); Fong and Srour (1994); Rosenthal and Stevens (1994); Carnes and Morgan (1995); Srour and Robertson (1995); Wilson (1997); Eom et al. (1999); Lopez et al. (1999); Wellman (1999); Wellmann and Srour (1999); Young et al. (1999); Becker and Güdesen (2000); Depireux and Shamma (2000); Mays and Price (2000); Mays and Vu (2000).
Army Acoustic Computer Models: Goal: To determine point-to-point losses in acoustic transmission: a. Spherical spreading model b. Parabolic Equation (PE) model c. Fast field Program (FFP) d. Scanning Fast Field Program (SCAFFIP) e. Acoustic Multistream Propagation Program (AMPP) f. Acoustic Battlefield Decision Aid (ABFA) g. Turbulence spectral model Atmospheric turbulence and refraction effects influence the retrieval and interpretation of acoustic signals.	Smith (1989); Sparrow (1991); West et al. (1991); West et al. (1992); Auvermann and Goedecke (1993); Wilson (1993); Noble (1994); Auvermann et al. (1995); Noble and Marlin (1995); Kotiaho (1996); Goedecke et al. (1997); Wilson (1998ab); Goedecke et al. (2000); Wilson (2000); Wilson and Szeto (2000); Auvermann (2001).

Table A-2. The atmospheric physics of sound speed (based on Fleagle and Businger 1963).

Change in pressure (dp) over a unit cross-sectional area of a fluid containing a sound wave (i.e., between the plane of compression and plane of rarefaction): (A-1) $dp = -\rho\ ds\ \frac{dc}{dt}$	Ratio of pressure change to volume change for an adiabatic (or isentropic) process: (A-2) $\frac{dp}{d\alpha} = -\frac{c_p}{c_v}\frac{p}{\alpha}$
Equation of state (EOS) for an ideal gas: (A-3) $p\ \alpha = \frac{RT}{M}$, where $R = 8314.32\ J\ mol^{-1}K^{-1}$ is the universal gas constant and M is molecular mass.	Speed of sound in air: (A-4) $c = \sqrt{\frac{\gamma\ RT}{M}}$, (A-5) $\gamma = \frac{c_p}{c_v} \sim 1.403$ is the ratio of specific heats. (A-6) c_o = 331.29 ms^{-1} is the reference value for speed of sound for standard dry air at 0 °C and a barometric pressure of 1013.25 mb (Wong 1986).
Ratio of specific heats and molar mass: (A-7) $\frac{\gamma}{M} = 0.04833 + (h - 0.023)A_t$, $A_t = 9.2\ x\ 10^{-5} + 5.5\ x\ 10^{-6}t\ +\ 4.25\ x\ 10^{-7}t^2$, h is humidity (in the range 0.0 to 1.0), and t is air temperature in degrees Celsius (Wong and Embleton 1984, 1985)	Effective sound speed **(Figure 1)**: (A-8) $c_{eff} = c_o + \bar{u}\ \cos\left(\theta_w - \pi - \theta_{S,R}\right)$, where c_{eff} accounts for increases (decreases) of sound speed due to variations in wind velocity (Noble and Marlin 1995 and Osteshev 1997)

Table A-3. Vertical profiles of wind speed in forests.

The study of winds in forests: A. To better understand the surface layer exchanges of heat, moisture (water vapor), and carbon dioxide, which not only influence regional and local climate, but also affect the forest ecosystem for growth and regeneration; B. For the study of transport, diffusion, and deposition of air-borne pollutants, trace gases, and aerial sprays; C. To assess the impact of wind damage on trees and tree harvests by severe storms.	
Survey of the literature:	
A. Meteorological measurements;	Allen (1968); Bergen (1971); Martin (1971); Oliver (1971); Raynor (1971); Denmead and Bradley (1985); Amiro and Davis (1988); Baldocchi and Hutchinson (1988); Baldocchi and Meyers (1988); Lee and Black (1995).
B. Model forests in wind tunnels;	Meroney (1968); Sadeh et al. (1971); Chen et al. (1995).
C. Atmospheric computer models of varying complexity.	Monin and Obukhov (1954); DeMarrais (1959); Inoue (1963); Cionco (1965); Barr (1971); Shinn (1971); Busch (1973); Dyer (1974); Benoit (1977); Shaw (1977); Touma (1977); Wilson and Shaw (1977); Irwin (1979); Garratt (1980, 1992); Albini (1981); Shaw and Periera (1982); Yamada (1982); Meyers and Paw U (1986); Meyers (1987); Wilson (1988); Paw U and Meyers (1989); Li et al. (1990); Shaw and Schumann (1992); Kaimal and Finnegan (1994); Zoumakis (1993, 1994); Finnegan and Brunet (1995); Lo (1995); Massman (1982); Shen and Leclerc (1997); Katul and Albertson (1998); Meyers et al. (1998); Wilson et al. (1998); Wilson and Flesch (1999); Pyles et al. (2000); Albertson et al. (2001); Li (2001); Pinard and Wilson (2001).
Main features of wind speed profile structure (**Figure 2**): 1) A low-level wind maximum at ~0.1 to 0.3h, where h is the height of the canopy top; 2) A layer of minimum wind speed at ~0.6 to 0.8h, which coincides with the region of maximum leaf area density; 3) A diurnal time maximum of wind speed, which extends through the entire canopy in the early afternoon.	

Table A-4. Wind speeds above a uniform forest stand.

Equations for (idealized) steady state, homogeneous, equilibrium conditions	Annotation	Reference
A. Wind flow with constant shearing stress: (A-9) $\frac{\partial \overline{U}}{\partial z} = \frac{u_*}{k(z-d)}\phi_m$ (A-10) $\overline{U} = \frac{u_*}{k}\left[\ln\left(\frac{z-d}{z_0}\right) - \psi_m\right]$	$\overline{U}$ is the mean wind speed; $u_* = \sqrt{\frac{\tau}{\rho}}$ is the friction velocity; $\frac{\tau}{\rho} = \overline{u'w'}$ is the shearing stress; ρ is air density; k is Karman's constant, $k \approx 0.4$; d is zero-plane displacement; z_0 is surface roughness length; ϕ_m is a function of stability; and ψ_m is the diabatic influence function.	Monin and Obukhov (1954); Panofsky (1963); Paulson (1970); Webb (1970); Busch (1973); Dyer (1974); Benoit (1977).
B. Power-law exponent model (A-11) $\overline{U}_{z_2} = \overline{U}_{z_1}\left(\frac{z_2-d}{z_1-d}\right)^P$	$\overline{U}_{z_1}$ and $\overline{U}_{z_2}$ are the wind speeds at heights z_1 and z_2 above h, the canopy top and the exponent p is a function of wind speed and stability.	DeMarrais (1959); Martin (1971) Touma (1977); Irwin (1979).
C. Windflow within the transition layer (i.e., $H \le z < z_*$): (A-12) $\frac{\partial \overline{U}}{\partial z} = \frac{u_*}{k(z-d)}\ \phi_m\ \phi_m^*$ (A-13) $\phi_m^* = \exp\left[-0.7\left(1-\frac{z}{z_*}\right)\right]$ (A-14) $\overline{U} = \frac{u_*}{k}\left[\ln\left(\frac{z-d}{z_0}\right) - \psi_m + \psi_m^*\right]$	Within the transition layer, additional momentum is transferred to the winds due to surface (canopy-top) generated eddies, which effectively decreased the vertical profile gradient **(Figure 4)**. z_* is the depth of the transition layer. z_* ~ 3 δ where δ is tree spacing, or z_* = 1.5h to 2.5h, depending on the roughness density. ψ_m^* is defined in the same manner as ψ_m.	Garratt (1980, 1992); Zoumakis (1993,1994); Kaimal and Finnegan (1994); Arya (2001).

Table A-5. Wind speed profile structure within a uniform forest stand.

Equations for (idealized) steady state, homogeneous, equilibrium conditions	Annotation	Reference
From conservation of momentum: (A-15) $\frac{\partial \overline{u'w'}}{\partial z} = -\frac{\partial p}{\partial x} - \frac{1}{2}C_d A \overline{U}^2$, a. Momentum flux divergence, b. Horizontal pressure gradient, and c. Drag due to friction imparted by the leaves and branches. This yields, (A-16) $\frac{\partial \overline{u'w'}}{\partial z} = -\frac{1}{2}C_d A \overline{U}^2$	$C_d = \frac{2u_*^2}{\overline{U}^2}$ is the surface drag coefficient A is the leaf area density per unit surface area of ground below. $LAI = \int_0^h A(z)\, dz$ is leaf area index; Generally, LAI = 1 to 5 for forests. Under conditions that the accelerations due to turbulent shearing stresses and drag forces in the upper part of the canopy are dominant (e.g., far enough away from leading or trailing edge transition zones) then equation (A-16) holds.	Barr (1971); Shaw (1977); Wilson and Shaw (1977). Pielke (1984); Kaimal and Finnigan (1994); Finnigan and Brunet (1995).
Upon integration, equation (A-16) yields, (A-17) $\overline{U} = \overline{U}_h \exp\left[-n\left(1 - \frac{z}{h}\right)\right]$	$\overline{U}_h$ is the mean wind speed at the forest top, $n = h\left(\frac{C_d A}{4l^2}\right)^{\frac{1}{3}}$ is the extinction coefficient or canopy flow index, and l is mixing length, i.e., $\overline{u'w'} = -l^2\left\lvert\frac{\partial \overline{U}}{\partial z}\right\rvert\frac{\partial \overline{U}}{\partial z}$.	Inoue (1963); Cionco (1965); Shinn (1971); Albini (1981).
Alternately, (A-18) $\overline{U} = \overline{U}_h \exp\left[-\lambda\left(1 - \frac{z}{h}\right)^{\beta}\right]$	$\lambda = LAI$, $\beta = 1 - \left(\frac{P-1}{4}\right)$, and P = 1, 2, or 3 correspond to one of the three general profile shapes (leaf area distributions) for forest canopies **(Figure 3)**.	Paw U and Meyers (1989); Meyers et al. (1998).
The subcanopy wind velocity components: (A-19) $\overline{u} = \overline{U}\sin\alpha_0$ (A-20) $\overline{v} = \overline{U}\cos\alpha_0$	$\alpha_0 = \tan^{-1}\left(\frac{\overline{v}}{\overline{u}}\right)$ is the subcanopy wind-turning angle	Shinn (1971).

Table A-6. Zero-Plane displacement, roughness length, and subcanopy wind maxima.

Equations for (idealized) steady state, homogeneous, equilibrium conditions	Annotation	Reference
Minimum wind speeds through the tree crown have been associated with the zero-plane displacement height, (A-21) $d = h\left(0.05+\frac{LAI^{0.2}}{2}+\frac{(P-1)}{20}\right)$	*LAI* is the leaf area index and P = 1, 2, or 3 correspond to one of the three general profile shapes for forest canopies. From various experiments in pine forests, $d \sim 0.70 - 0.76h$.	Shaw and Periera (1982); Meyers (1987); Paw U and Meyers (1989); Meyers et al. (1998). Bergen (1971); Raynor (1971); Oliver (1971); Lee and Black (1993).
Surface (aerodynamic) roughness (in equation A-10) has been parameterized in the following manner: (A-22) $z_0 = h\left(0.23-\frac{LAI^{0.25}}{10}-\frac{(P-1)}{67}\right)$	Roughness (z_0) varies in the following manner: ~ 10^{-4} m over snow, sand, dry lakebeds; ~ 10^{-2} m over soils; ~ 0.1 m over farmlands, tall grass, or shrubs; ~ 1.0 m for orchards and forests.	Oke (1978); Pielke (1984); Rachele and Tunick (1994).
Through the open trunk spaces where air flow is considerable less restricted, equation (A-15) yields (A-23) $0 = -\frac{\partial p}{\partial x} - \frac{1}{2}C_d A \overline{U}^2$ 1) Wind speeds are mainly influenced by drag at the ground surface, thermal stability, wind gusts that penetrate through clearings at the forest top, and to a lesser extent (in a large uniform expanse), horizontal advection; 2) A low-level wind maximum is often observed at a height around the base of the live branches, the magnitude of which is strongly influenced by the forest type and leaf area density; 3) The turbulent wind shearing stress may be depleted because momentum is absorbed most strongly through the upper canopy layers (i.e., within the crown); 4) As a result, the low-level wind speed maximum occurs in a transition layer between the upper-canopy extinction type profile and the log-law type profile that we would expect extends from this height to the ground.		Shinn (1971); Shaw (1977); Shaw et al. (1974); Holland (1989).

Table A-7. First-Order closure models and higher-order closure models to include large eddy simulations.

Equations	Reference
Continuity (Conservation of Matter): (A-24) $\frac{\partial \overline{u_j}}{\partial x_j} = 0$ Equation for the Mean Flow: (A-25) $\frac{\partial \overline{u_i}}{\partial t} + \overline{u_j}\frac{\partial \overline{u_i}}{\partial x_j} + \frac{\partial \overline{u_i'u_j'}}{\partial x_j} = \frac{\partial \overline{p}}{\partial x_i} - \overline{\frac{\partial p'}{\partial x_i}} + \nu \frac{\partial^2 \overline{u_i}}{\partial^2 x_j} + \nu \overline{\frac{\partial^2 u_i'}{\partial^2 x_j}}$ a. Time tendency of the winds, b. Advection of the mean wind, c. Momentum flux divergence, d. Mean pressure gradient, e. Pressure drag force, f. Viscous drag force on the mean flow, and g. Viscous drag force from the canopy elements. When the mean pressure gradient is considered negligible, and pressure drag forces are considered the main portion of the total drag from the forest canopy, the following closure assumption is often used (A-26) $\overline{\frac{\partial p'}{\partial x_i}} = C_d A \overline{u_i}^2$	Wilson and Shaw (1977); Yamada (1982); Wilson (1988); Meyers and Paw U (1986); Meyers (1987); Paw U and Meyers (1989); Shaw and Schumann (1992); Shen and Leclerc (1997); Katul and Albertson (1998); Pyles et al. (2000); Albertson et al. (2001); Li (2001).
First-order turbulence closures for the momentum flux divergence: (A-27) $\frac{\partial \overline{u_i'u_j'}}{\partial x_j} = \frac{\partial}{\partial x_j} K_{(ij)} \left(\frac{\partial \overline{u}_i}{\partial x_j} + \frac{\partial \overline{u}_j}{\partial x_i} \right)$ where (A-28) $K_{(ij)} = l^2 \sqrt{\left(\frac{\partial \overline{u}_i}{\partial x_j} \right)^2 + \left(\frac{\partial \overline{u}_j}{\partial x_i} \right)^2}$ Alternately, (A-29) $K = \lambda_{mix} \left(\frac{u_*^2}{tke(h)} tke(z) \right)^{\frac{1}{2}}$ where $tke = \frac{1}{2}\sum u_i'^2$ and $\frac{u_*^2}{tke(h)}$ is the ratio of the equilibrium shearing stress and turbulent kinetic energy at the forest canopy top.	Li et al. (1990); Wilson et al. (1998); Wilson and Flesch (1999); Pinard and Wilson (2001).

Table A-8. Vertical profiles of temperature in forests.

Equations	Reference
The conservation of energy (or enthalpy, $c_p\overline{\theta}$) equation: (A-30) $\frac{\partial\overline{\theta}}{\partial t} + \overline{u}_j\frac{\partial\overline{\theta}}{\partial x_j} = -\frac{\partial\left(\overline{u_j'\theta'}\right)}{\partial x_j} + \kappa_T\frac{\partial^2\overline{\theta}}{\partial x_j^2} + \frac{1}{\rho\, c_P}\frac{\partial\overline{R}_j}{\partial x_j}$ a. Time tendency of the mean potential temperature ($\overline{\theta}$); b. Advection of potential temperature by the mean wind; c. Eddy heat flux divergence; d. Viscous dissipation of heat; e. Net radiative flux divergence through the forest canopy.	Businger (1982); Garratt (1992).
(A-31) $\frac{\partial\left(\overline{w'\theta'}\right)}{\partial z} \propto n\left(T_a - T_f\right)A$ where n is the heat transfer coefficient for the leaf (pine needle) surface, T_a is the air temperature, T_f is the leaf (needle) surface temperature, and A is the foliage surface area in the volume. $\left(T_a - T_f\right)$ will depend on: a. Solar altitude; b. Ratio of diffuse to direct solar radiation; c. Cloud cover; and d. Angle between the wind velocity at the canopy top and the solar azimuth.	Bayton (1963); Munn (1966); Raynor (1971); Bergen (1974); Hosker et al. (1974) Denmead and Bradley (1985); Huisman and Attenborough (1991); Fontan et al. (1992); Lee et al. (1997).

Main features of temperature profile structure within and above forests, **Figures (5) and (6)**:

1) Inversion conditions during the day and isothermal or slightly unstable lapse conditions at night;
2) Inversion conditions will sometimes develop during the daytime above forests due to evaporative cooling from leaf transpiration;
3) Temperature profiles above forests will not normally maintain large (positive or negative) gradients;
4) The forest canopy captures incoming solar radiation and a layer of warm air develops that propagates downward through normal mixing processes;
5) Maximum temperatures are shown to coincide with the height of maximum leaf density (and minimum wind speeds);
6) A local minimum in temperature occurs through the trunk space below the live branches;
7) Under cloudy conditions (with and without rainfall), mostly isothermal conditions have been observed within a pine forest canopy throughout the day;
8) At night, the forest canopy loses heat and is cooled further (from the upper crown area downward) by subsidence so that isothermal conditions (or sometimes weak negative lapse rate conditions) prevail;
9) A second inversion is likely to form close to the ground at night due to surface (radiative) cooling of the soil; and
10) Intermittent wind gusts through openings at the top of the forest canopy often bring downdrafts of cooler and drier air from above into the canopy and subcanopy layers.

Table A-9. Observed short-range acoustic attenuation in forests.

Parameters	Reference
Attenuation of sound waves in forests is said to involve three main phenomena: 1) Interference between direct and ground reflected acoustic waves; 2) Scattering by tree trunks and branches, the ground, and turbulence; and 3) Absorption by the trees, leaves, branches, the ground, and the air Ground impedance, which affects sound-wave reflection and absorption, is a function of flow resistivity and surface porosity. σ = 20–80 kPa s m^{-2} is flow resistivity for forest stands; σ = 150–300 kPa s m^{-2} is flow resistivity for grass; σ = 300–800 kPa s m^{-2} is flow resistivity soil covered surfaces. Ω = 0.825 is the porosity for the forest floor, which consists of humus, leaves (needles), and other biological litter; Ω = 0.675 is the porosity for grass fields; and Ω = 0.575 is the porosity for unpacked soils. • Ground impedance affects sound attenuation mainly in the mid 250–500 Hz frequency range. • At higher frequencies ($f \geq$ 1–2 kHz), sound attenuation in forests is mainly due to scattering by tree trunks and branches and absorption by foliage. • Such phenomena may have a greater effect on sound attenuation at higher frequencies than refraction effects due to temperature inversions and wind speeds in the forest canopy.	Erying (1946); Embleton (1963); Aylor (1972); Burns (1979); Embleton et al. (1983); Fricke (1984); Attenborough (1985); Price et al. (1988); Huismann and Attenborough (1991); Sakai et al. (1998, 2001).

REPORT DOCUMENTATION PAGE

Form Approved
OMB No. 0704-0188

1. AGENCY USE ONLY *(Leave blank)*	2. REPORT DATE	3. REPORT TYPE AND DATES COVERED
	September 2002	Final, October 2001 to January 2002

4. TITLE AND SUBTITLE
Coupling Meteorology to Acoustics in Forests

5. FUNDING NUMBERS
DA PR: AH71
PE: 62784A

6. AUTHOR(S)
Arnold Tunick

7. PERFORMING ORGANIZATION NAME(S) AND ADDRESS(ES)
U.S. Army Research Laboratory
Attn: AMSRL- CI-EE
2800 Powder Mill Road
Adelphi, MD 20783-1197

8. PERFORMING ORGANIZATION REPORT NUMBER
ARL-MR-538

9. SPONSORING/MONITORING AGENCY NAME(S) AND ADDRESS(ES)
U.S. Army Research Laboratory
2800 Powder Mill Road
Adelphi, MD 20783-1197

10. SPONSORING/MONITORING AGENCY REPORT NUMBER

11. SUPPLEMENTARY NOTES
ARL PR: 2FEH26
AMS code: 622784H7111

12a. DISTRIBUTION/AVAILABILITY STATEMENT
Approved for public release; distribution unlimited.

12b. DISTRIBUTION CODE

13. ABSTRACT *(Maximum 200 words)*

The U.S. Army has a growing interest in the use of advanced sensors and computer models to retrieve, display, and interpret acoustic signals from sound-emitting targets in and around forests. Outdoor sound speed is an essential parameter for determining point-to-point acoustic propagation. The speed of sound is often expressed as a function of air temperature, humidity, and wind velocity. Therefore, we have reviewed selected past research on micrometeorology within and above forests to examine the calculation of the speed of sound through the atmosphere in the forest environment for military acoustic applications. Our objective is to evaluate meteorological models for estimating wind speed and temperature profiles within and above forests to determine those most applicable in representing mechanical and thermodynamic influences on the speed of sound in the forest environment.

14. SUBJECT TERMS	15. NUMBER OF PAGES
sound propagation, computer model, speed of sound, micrometeorology	47
	16. PRICE CODE

17. SECURITY CLASSIFICATION OF REPORT	18. SECURITY CLASSIFICATION OF THIS PAGE	19. SECURITY CLASSIFICATION OF ABSTRACT	20. LIMITATION OF ABSTRACT
Unclassified	Unclassified	Unclassified	UL

NSN 7540-01-280-5500

Standard Form 298 (Rev. 2-89)
Prescribed by ANSI Std. Z39-18
298-102